Title

Fibroblast Growth Factor Receptors Function Redundantly During Zebrafish Embryonic Development.

Journal

Genetics, 212(4)

ISSN

0016-6731

Authors

Leerberg, Dena M
Hopton, Rachel E
Draper, Bruce W

Publication Date

2019-08-01

DOI

10.1534/genetics.119.302345

Peer reviewed

Fibroblast Growth Factor Receptors Function Redundantly During Zebrafish Embryonic Development

Dena M. Leerberg,[1] Rachel E. Hopton,[2] and Bruce W. Draper[3]
Department of Molecular and Cellular Biology, University of California, Davis, California 95616
ORCID IDs: 0000-0001-9731-998X (D.M.L.); 0000-0002-4397-7749 (B.W.D.)

ABSTRACT Fibroblast growth factor (Fgf) signaling regulates many processes during development. In most cases, one tissue layer secretes an Fgf ligand that binds and activates an Fgf receptor (Fgfr) expressed by a neighboring tissue. Although studies have identified the roles of specific Fgf ligands during development, less is known about the requirements for the receptors. We have generated null mutations in each of the five *fgfr* genes in zebrafish. Considering the diverse requirements for Fgf signaling throughout development, and that null mutations in the mouse *Fgfr1* and *Fgfr2* genes are embryonic lethal, it was surprising that all zebrafish homozygous mutants are viable and fertile, with no discernable embryonic defect. Instead, we find that multiple receptors are involved in coordinating most Fgf-dependent developmental processes. For example, mutations in the ligand *fgf8a* cause loss of the midbrain-hindbrain boundary, whereas, in the *fgfr* mutants, this phenotype is seen only in embryos that are triple mutant for *fgfr1a;fgfr1b;fgfr2*, but not in any single or double mutant combinations. We show that this apparent *fgfr* redundancy is also seen during the development of several other tissues, including posterior mesoderm, pectoral fins, viscerocranium, and neurocranium. These data are an essential step toward defining the specific Fgfrs that function with particular Fgf ligands to regulate important developmental processes in zebrafish.

KEYWORDS Fibroblast growth factor signaling; posterior mesoderm; pectoral fin; midbrain-hindbrain boundary; viscerocranium; neurocranium

THE coordination of cellular events that drive developmental processes requires robust communication between cells. One common communication mechanism is the Fibroblast growth factor (Fgf) signaling pathway, which involves a diffusible Fgf ligand that is secreted into the extracellular space, where it interacts with heparan sulfate and an Fgf receptor (Fgfr) (reviewed in Mohammadi *et al.* 2005). Fgfrs are single-pass transmembrane proteins composed of an extracellular region containing immunoglobulin (Ig) domains and an intracellular tyrosine kinase domain. Upon ligand binding, receptor dimerization leads to transphosphorylation-dependent activation of the kinase domain (Lemmon and Schlessinger 1994). Fgf signaling can activate several intracellular signal transduction pathways, including the MAPK, PLCγ, and PI3K/Akt cascades (Pawson 1995). While Fgf signaling can result in transcriptional changes, the ultimate cellular response depends on context and ranges from proliferation to migration and differentiation (reviewed in Powers *et al.* 2000).

Although the Fgf signaling pathway likely arose in eumetazoans (Bertrand *et al.* 2014), the Fgf ligand and receptor gene repertoire has increased in more complex animals. For example, the mammalian genome contains 22 ligand and four receptor genes, and the zebrafish genome has 31 ligand and five receptor genes (Ornitz and Itoh 2001). These genes are expressed widely throughout both developing and mature tissues, often in overlapping domains (Sleptsova-Friedrich *et al.* 2001; Thisse *et al.* 2001, 2008; Tonou-Fujimori *et al.* 2002; Scholpp *et al.* 2004; Nechiporuk *et al.* 2005; Thisse and Thisse 2005; Harvey and Logan 2006; Rohner *et al.*

doi: https://doi.org/10.1534/genetics.119.302345
Manuscript received December 20, 2018; accepted for publication May 29, 2019; published Early Online June 7, 2019.
Available freely online through the author-supported open access option.
Supplemental material available at FigShare: https://doi.org/10.25386/genetics.8162003.
[1]Present address: Section of Cell and Developmental Biology, University of California, San Diego, La Jolla, CA 92093.
[2]Present address: Institute of Molecular Biology, University of Oregon, Eugene, OR 97403.
[3]Corresponding author: Department of Molecular and Cellular Biology, University of California, Davis, 149 Briggs Hall, One Shields Ave., Davis, CA 95616. E-mail: bwdraper@ucdavis.edu

2009; Camarata *et al.* 2010; Ota *et al.* 2010; Larbuisson *et al.* 2013; Rohs *et al.* 2013; Koch *et al.* 2014; Lovely *et al.* 2016). Tissue culture-based experiments have indicated that individual Fgf ligands have some degree of preference for the receptors they activate (Ornitz *et al.* 1996). This preference seems to be conferred by interactions between the glycine box, a ~10 AA stretch near the C-terminus of an Fgf ligand (Luo *et al.* 1998), and the third Ig domain (IgIII) of the receptors (Johnson *et al.* 1991; Yayon *et al.* 1992). Interestingly, FGFR1, FGFR2, and FGFR3 in mammals, and Fgfr1a and Fgfr2 in zebrafish, are subject to alternative splicing in this IgIII domain, and these alternative isoforms have different affinities for particular ligands (Johnson *et al.* 1991; Werner *et al.* 1992; Chellaiah *et al.* 1994; Yeh *et al.* 2003).

Previously, studies have investigated the roles of Fgf signaling by disrupting the function of particular ligands. In zebrafish alone, the function of many Fgf ligands during early development has been determined using genetic mutation or morpholino (MO) knockdown. In some cases, disrupting a single Fgf gene leads to a developmental defect. For example, disrupting *fgf24*, *fgf10a*, or *fgf16* signaling results in the absence of pectoral fins, whereas loss of *fgf8a* leads to midbrain-hindbrain boundary (MHB) defects (Brand *et al.* 1996; Reifers *et al.* 1998; Fischer *et al.* 2003; Nomura *et al.* 2006; Manfroid *et al.* 2007). In other contexts, however, Fgf ligands appear to function redundantly. While both *fgf8a* and *fgf24* single mutants have normal mesoderm development, disrupting both ligands simultaneously leads to loss of posterior mesodermal derivatives and a consequent shortening of the embryonic axis (Draper *et al.* 2003). Similarly, simultaneous loss of both *fgf8a* and *fgf3* leads to severe defects in pharyngeal pouch development, whereas this tissue develops normally in either single mutant (Crump *et al.* 2004a; McCarthy *et al.* 2016). These and similar data suggest that genetic redundancy in the Fgf signaling components creates a robust developmental system (Brand *et al.* 1996; Reifers *et al.* 1998; Draper *et al.* 2003; Fischer *et al.* 2003).

In contrast to the known requirements of many Fgf ligands during development, comparatively less is known about the requirements for specific Fgfrs. In the mouse, null mutation of *Fgfr1* or *Fgfr2* is embryonic lethal (Deng *et al.* 1994; Yamaguchi *et al.* 1994; Arman *et al.* 1998), whereas tissue-specific disruption of these genes reveals their roles during later development in limbs and/or brain (Xu *et al.* 1998, 1999a; Trokovic *et al.* 2003). By contrast, *Fgfr3* and *Fgfr4* homozygous mutants are embryonic viable, though *Fgfr3* single mutants have skeletal dysplasia, and *Fgfr3*;*Fgfr4* double mutants have defective lung development. These latter results suggest that, like certain Fgf ligands, Fgf receptors also function redundantly in some developmental contexts (Colvin *et al.* 1996; Deng *et al.* 1996; Weinstein *et al.* 1998). The zebrafish genome contains single copies of *fgfr2-4* orthologs, and two copies of an *fgfr1* ortholog, called *fgfr1a* and *fgfr1b*, that appear to have arisen during the teleost-specific whole genome duplication (Rohner *et al.* 2009). In contrast to several *fgf* ligand mutants, which have been isolated in phenotype-based forward genetic screens for recessive mutations, only one mutation in an Fgf receptor has been identified in a recessive screen—a result that could be explained if Fgf receptors function redundantly, an idea supported by the extensive spatial overlap of Fgfr gene expression in zebrafish embryos (Reifers *et al.* 1998; Fischer *et al.* 2003; Norton *et al.* 2005). The one exception is *fgfr1a*, where a point mutation in the kinase domain, proposed to be a strong hypomorph, is embryonic viable, but has defects in scale formation during juvenile development (Rohner *et al.* 2009).

To determine the precise requirements of each Fgf receptor during embryonic development, we have produced loss-of-function mutations in each of the five zebrafish *fgf* receptor genes. Because of the known requirements for Fgf signaling during early zebrafish development, we expected that some of the receptor mutants would phenocopy known Fgf ligand mutants. However, we found that all single mutants are viable with no overt embryonic phenotypes; instead, we discovered that only certain double and triple mutant combinations have developmental defects in the posterior mesoderm, brain, pectoral fin, and pharyngeal arch derived cartilages. These findings suggest significant genetic redundancy between various Fgf receptors, and indicate that some ligands are capable of activating signaling through as many as three different receptors.

Materials and Methods

Husbandry

The wild-type strain *AB was used for the generation of *fgfr3*^{uc51} *and fgfr4*^{uc42}. The wild-type strain NHGRI-1 was used for the generation of *fgf1a3*^{uc61}, *fgfr1b*^{uc62}, and *fgfr2*^{uc64}. Zebrafish husbandry was performed as previously described (Westerfield 2000; Leerberg *et al.* 2017).

Generation of alleles

For *fgfr3*^{uc51} and *fgfr4*^{uc42}, sgRNAs were designed using ZiFiT. Two oligonucleotides (see Supplemental Material, Table S1) were annealed and cloned into plasmid pDR274 (Addgene Plasmid #42250). For *fgfr1a*^{uc61}, *fgfr1b*^{uc62}, and *fgfr2*^{uc64}, sgRNAs were designed using CRISPRscan (Moreno-Mateos *et al.* 2015) and produced as described (Shah *et al.* 2016). Briefly, overlap PCR of a T7 RNA promoter containing a gene-specific oligonucleotide and a PAGE-purified scaffold oligonucleotide (see Table S1) was used to generate the DNA template for *in vitro* transcription. *cas9* mRNA was produced using the pT3TS-nls-zCas9-nls containing a codon-optimized Cas9 with two nuclear localization sequences as described in Jao *et al.* (2013). The plasmid was linearized with *Xba*I and transcribed using the mMESSAGE mMACHINE T3 Transcription Kit (Cat. No. AM1348; Thermo Fisher). The sgRNA and *cas9* mRNA were co-injected into one-cell embryos with phenol red (5% in 2 M KCl) at concentrations of 60 ng/μl and 30 ng/μl, respectively.

CRISPR efficiency was determined by comparing the targeted loci of eight injected embryos and eight control embryos

[24 hr postfertilization (hpf)] by High Resolution Melt Analysis (HRMA) as described (Dahlem *et al.* 2012) (see Table S2 for primers used). Germline mutations were identified by PCR analysis of sperm DNA from injected males (see Table S2 for primers used). Indels were sequenced, and individuals containing frameshift inducing indels were outcrossed to *AB or NHGRI-1 to obtain F1s. To reduce the potential for off-target effects, all lines were outcrossed at least four times prior to analysis.

Genotyping

Genomic DNA was extracted from caudal fin tissue. Genotypes were determined using standard PCR conditions (*fgfr1a*^{uc61}, *fgfr1b*^{uc62}, *fgfr2*^{uc64}, and *fgfr3*^{uc51}) or HRMA (*fgfr4*^{uc42}), and primers listed in Table S2.

RNA in situ hybridization

RNA probes that detect the following genes were used: *ta* (Schulte-Merker *et al.* 1992); *myod* (Begemann and Ingham 2000); *pax2a* (Krauss *et al.* 1991); *tbx5a* (Begemann and Ingham 2000); *fgf24* (Draper *et al.* 2003); *etv4* (Münchberg *et al.* 1999); *fgf8a* (Reifers *et al.* 1998). For *has2*, *dlx2a*, *alcama*, *fgf10a*, and *en2a* probe synthesis, mRNA was isolated from 24 hpf embryos using TRI reagent (Cat. No. T9424; Sigma-Aldrich) and synthesized into cDNA using the RETROScript Reverse Transcription Kit (Cat. No. AM1710; ThermoFisher). DNA templates for *in vitro* transcription were PCR amplified with Phusion polymerase (Cat. No. M0530L; New England BioLabs) and the primers listed in Table S3. Reverse primers contained a T7 RNA polymerase promoter (Table S3, underlined portion), and *in vitro* transcription yielded antisense probes (Roche T7 RNA polymerase, Cat. No. 10881775001). Probes were purified with the RNA Clean and Concentrator kit (Cat. No. R1015; Zymo) and G-50 sephadex columns (Cat. No. 45-001-398; GE Healthcare). Probes were used at a concentration of 0.5–2 ng/μl in hybridization solution.

Samples were fixed in 4% paraformaldehyde (PFA) overnight at 4° or 4 hr at room temperature. Samples were dehydrated with 100% methanol and stored at −20° for at least 16 hr. Embryos >30 hpf were bleached for ~10 min prior to proteinase K digestion in 3% H_2O_2, 0.5% KOH. Color *in situ* hybridizations were performed by a procedure similar to that of Thisse *et al.* (2008), with the exception that 5% dextran sulfate was included in the hybridization solution.

Bone and cartilage stains

For the scale stain depicted in Figure S2, adults were fixed in 4% PFA for 3 days, followed by 3 × 30 min rinses in deionized water. Samples were bleached with 0.5% H_2O_2/1% KOH to remove pigment, and scales were stained with 1% alizarin red/1% KOH. Cartilage stains in Figure 6 and Figure 7 were performed as previously described (Walker *et al.* 2006).

Imaging

Embryos were mounted in 4% methylcellulose and imaged on a Leica MZ16 F stereomicroscope. Embryos in Figure 3, E–G were flat-mounted in 70% glycerol and imaged on a Zeiss Axiophot microscope. Images were collected with a Leica DFC500 digital camera.

RT-qPCR

For RT-qPCR experiments, tail biopsies were collected from 24 hpf embryos and placed immediately in genomic DNA lysis buffer (10 mM Tris pH 8.4, 50 mM KCl, 1.5 mM $MgCl_2$, 0.3% Tween-20, 0.3% NP-40). Bodies were collected in 1.6 ml microcentrifuge tubes and stored in liquid nitrogen until tail tissue could be genotyped using the primers listed in Table S2. Total RNA was isolated from the bodies according to (de Jong *et al.* 2010) with the following exceptions: disposable pestles (Cat. No. 1415–5390; USA Scientific) were used in lieu of metal; Tri Reagent (Cat. No. AM9738; Thermo Fisher Scientific) in lieu of Qiazol; 100 μl of chloroform was added to homogenate instead of 60 μl; vacuum grease was used in lieu of phase lock gel heavy; RNA Clean and Concentrator with on-column DNase treatment (Cat. No. R1014; Zymo Research) in lieu of RNeasy MinElute Cleanup; RNA was eluted with 8.5 μl nuclease-free water instead of 14 μl. RNA was quantified using a NanoDrop 1000 (Thermo Fisher Scientific). cDNA libraries were prepared using 200 ng of total RNA in a 10 μl reaction using the RETROscript Reverse Transcription Kit (Cat. No. AM1710; Thermo Fisher Scientific), and diluted 1:5 after reverse transcription.

qPCR reactions (20 μl) were prepared with SsoAdvanced Universal SYBR Green Supermix (Bio-Rad), 1 μl of diluted cDNA, and primers (final concentration: 0.25 μM) listed in Table S4. Only primer sets with a PCR efficiency between 1.9 and 2.1, and an R^2 value above 0.98 were used for qPCR experiments. Reactions were performed on a Bio-Rad CFX96 machine with three technical replicates. Samples whose technical replicates had a standard deviation (SD) >0.26 cycles were discarded. Fold change between wild-type and mutant animals was determined using the ddCt method and *rpl13a* as the reference gene. Unpaired Student's *t*-tests were performed to determine whether the expression of individual *fgfr* genes changed between wild-type and mutant siblings (*e.g.*, expression of *fgfr1b* in wild type compared to *fgfr1a*$^{-/-}$ mutants). MANOVA tests were performed to determine whether the combined changes in wild-type *fgfr* mRNAs were significantly different between wild-type and mutant siblings (*e.g.*, combined expression of *fgfr2*, *fgfr3*, and *fgfr4* in wild-type compared to *fgfr1a*$^{-/-}$;*fgfr1b*$^{-/-}$ mutants).

Statistics and plotting

Statistics were performed in R and RStudio, using standard packages (R Core Team 2015). Graphing was performed in R, using ggplot2 (Wickham 2009).

Data availability

All fish lines and plasmids are available upon request. Fish lines will be deposited at the Zebrafish International Resource Center. Supplemental material available at FigShare: https://doi.org/10.25386/genetics.8162003.

Results and Discussion

Generation of mutant alleles

To determine the function of Fgf receptors in zebrafish development, we generated a null allele for each gene using the CRISPR/Cas9 gene editing system. Fgf receptors are composed of an extracellular ligand-binding domain, a single transmembrane domain, and an intracellular kinase domain. We used single-stranded guide RNAs to target Cas9 endonuclease to the 5′ end of each coding sequence to induce frameshift-causing indel mutations, which were confirmed by sequencing genomic DNA and then cDNA to assess the possibility of exon skipping that could result in a truncated, but functional, protein (Mou *et al.* 2017; Sharpe and Cooper 2017; Figure 1A and Table 1). A 127-bp insertion into *fgfr1a* exon 5 was the only mutation that resulted in exon skipping. However, because exon 5 is not a multiple of three (173 bp), the mis-spliced transcript goes out of frame at the aberrant splice junction. The predicted peptides that can be potentially translated from each of the five mutant alleles are illustrated in Figure 1A.

Fgf signaling is involved in many developmental processes, and all five *fgfr* genes are expressed during zebrafish embryogenesis (Sleptsova-Friedrich *et al.* 2001; Thisse *et al.* 2001; Tonou-Fujimori *et al.* 2002; Scholpp *et al.* 2004; Nechiporuk *et al.* 2005; Thisse and Thisse 2005; Harvey and Logan 2006; Thisse *et al.* 2008; Rohner *et al.* 2009; Camarata *et al.* 2010; Ota *et al.* 2010; Larbuisson *et al.* 2013; Rohs *et al.* 2013; Koch *et al.* 2014; Lovely *et al.* 2016; Figure 1B). It was therefore surprising that all five *fgfr* homozygous mutants were embryonic viable and had no apparent defects when compared to wild-type siblings (Figure 1, C–H). Because zygotic defects are often masked by maternally provided gene products (*e.g.*, Waskiewicz *et al.* 2002; Giraldez *et al.* 2005; Ciruna *et al.* 2006; Cheng *et al.* 2017; Hino *et al.* 2018), we asked if any of the Fgf receptor mRNAs are maternally provided, and found that, indeed, *fgfr1a* mRNA (specifically the splice isoform IIIc), and, to a lesser extent, *fgfr1b* RNA, are maternally provided (Scholpp *et al.* 2004; Rohner *et al.* 2009; Ota *et al.* 2010; Figure 1B). It was therefore possible that this maternal contribution could explain the absence of a phenotype when only the zygotic *fgfr* expression is lost. To test this, we produced maternal-zygotic (MZ) mutants, which are mutant embryos derived from homozygous mutant mothers, and, therefore, lack both maternal (M) and zygotic (Z) gene products. We found that MZ*fgfr1a* and MZ*fgfr1b* single mutant embryos were phenotypically wild-type (Figure S1). Thus, the absence of phenotypes for any of the receptor single mutants is not likely due to rescue by maternally provided gene products. These data also suggest that the receptor genes act in a redundant or compensatory manner during early development.

Previously, a point mutation in *fgfr1a*, called *fgfr1a(t3R05H)*, was shown to affect juvenile scale development in zebrafish

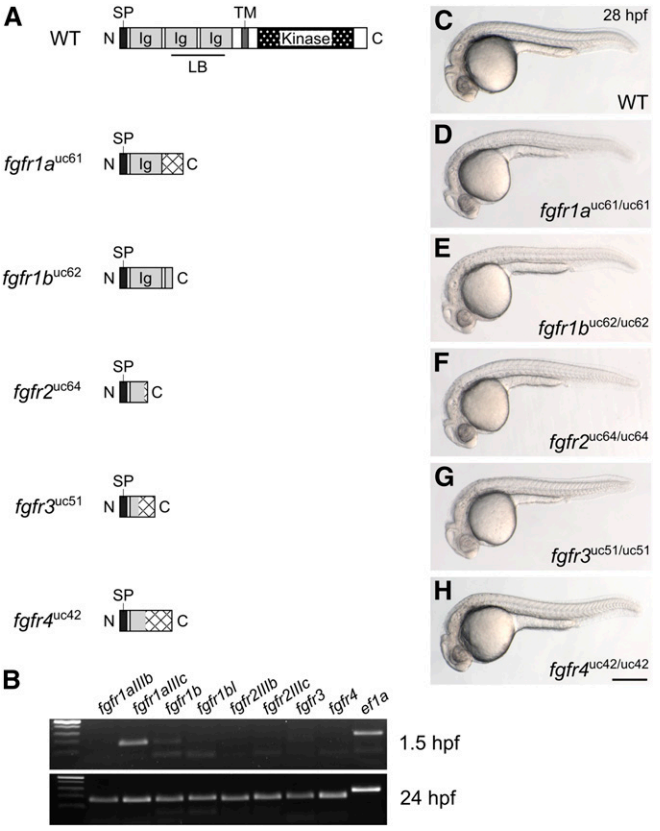

Figure 1 Fgf receptor mutants are embryonic viable. (A) Schematic diagram of a typical full-length Fgfr protein and the predicted truncated peptides resulting from the *fgfr1a*^{uc61}, *fgfr1b*^{uc62}, *fgfr2*^{uc64}, *fgfr3*^{uc51}, and *fgfr4*^{uc42} alleles. Hatching indicates missense amino acids. (B) RT-PCR of wild-type embryos. While all *fgfr* isoforms are detected in 24 hr postfertilization (hpf) embryos (postzygotic genome activation, bottom panel), only *fgfr1a* (isoform IIIc) and *fgfr1b* are detected in 1.5 hpf embryos (prezygotic genome activation, top panel). *ef1a* is shown as a positive control. (C–H) Lateral view of ~28 hpf wild-type (WT, C) or homozygous mutant (D–H) embryos. Anterior is to the left, dorsal is up. Bar in (H), 200 μm for (C–H). Ig, immunoglobulin; LB, ligand-binding domain; SP, signal peptide; TM, transmembrane domain.

(Rohner *et al.* 2009). Animals homozygous for this mutation, which affects a conserved arginine in the intracellular kinase domain and is predicted to be a strong hypomorph, develop with fewer flank scales, and the remaining scales are significantly larger than those of wild-type animals. We therefore asked if a similar scale phenotype in present in animals homozygous for *fgfr1a(uc61)* null mutations. Indeed, three of five *fgfr1a(uc61)* mutants analyzed had noticeably larger flank scales compared to wild-type siblings (dotted outlines, Figure S2). However, we did not observe the severe reduction in scale number reported for *fgfr1a(t3R05H)* mutants (Rohner *et al.* 2009), suggesting that the severity of this phenotype may be influenced by the genetic background. Alternatively, it is possible that *fgfr1a(t3R05H)* is a weak antimorph mutation, as it is known that overexpression of an Fgfr lacking a functional intercellular kinase domain can be dominant-negative (Amaya *et al.* 1991; Griffin *et al.* 1995).

Table 1 Nature of CRISPR/Cas9-generated alleles

Gene	Allele	Nature of genomic disruption	Exons skipped during splicing	WT peptide length (AA)	Predicted length of resulting peptide (AA)	# of AA in frame
fgfr1a	uc61	127 bp inserted into exon 5	Exon 5	810	202	138
fgfr1b	uc62	5 bp deleted from exon 6	—	741	220	220
fgfr2	uc64	47 bp deleted from exon 3	—	838	76	71
fgfr3	uc51	50 bp deleted from exon 3	—	821	95	49
fgfr4	uc50	4 bp deleted from exon 3	—	922	134	64

Genetic redundancy and transcriptional compensation in Fgf receptor mutants

Recently, it has been shown that indel alleles generated by genome editing technologies can result in phenotypes that are weaker than either point mutant alleles or MO oligo knockdown. This is likely due to a mechanism known as genetic compensation, where the transcription of a gene(s) related to the mutated gene is upregulated in mutants and functionally compensates, either partially or completely, for the mutated gene (Rossi *et al.* 2015; El-Brolosy *et al.* 2019; Ma *et al.* 2019). Given that the Fgf receptors share extensive sequence similarity, it was possible that transcriptional compensation could account for the lack of phenotype in our Fgfr mutants. To test this, we used reverse transcription quantitative real-time PCR (RT-qPCR) to examine the expression of all *fgfr* genes in our *fgfr* mutants. We compared *fgfr* gene expression between individual wild-type, single mutant, and select double and triple mutant 24 hpf embryos (Figure 2). Although expression changes are modest, trends emerge from our data. First, with one exception, the mRNA of the mutated gene is detected at significantly lower levels compared to wild type, suggesting that the mutant mRNAs are subject to nonsense-mediated decay (NMD). The exception to this is that, in comparison to wild-type controls, *fgfr2* mRNA is significantly decreased in $fgfr2^{-/-}$ single (Figure 2C) and $fgfr1a^{-/-};fgfr2^{-/-}$ double mutants (Figure 2G), but not in $fgfr1a^{-/-};fgfr1b^{-/-};fgfr2^{-/-}$ triple mutant embryos (Figure 2, H and I shows confirmation that these triple mutant embryos are indeed mutant for *fgfr2*). The reason for this is not known.

Given that NMD appears to induce transcriptional adaption (El-Brolosy *et al.* 2019; Ma *et al.* 2019), we tested whether our mutants have increased expression of the wild-type *fgfr* mRNAs. With the exception of *fgfr4* mutants, which have a significant increase in the expression of wild-type *fgfr2* and *fgfr3* mRNA (Figure 2E), none of the other single mutants displayed significant increases in the expression of any of the wild-type *fgfr* RNAs (Figure 2, A–D). By contrast, all double and triple mutant combinations we examined had significantly higher levels of wild-type *fgfr3* mRNA (in $fgfr1a^{-/-};fgfr1b^{-/-}$ and $fgfr1a^{-/-};fgfr1b^{-/-};fgfr2^{-/-}$ mutant combinations) or *fgfr4* mRNA (in $fgfr1a^{-/-};fgfr2^{-/-}$ mutants) when compared to wild-type controls (Figure 2, F–H). Whether these increases in wild-type *fgfr* mRNA expression in the double and triple mutants result in less severe mutant phenotypes remains to be determined. Importantly, because significant upregulation of any of the wild-type *fgfr* mRNAs in single mutants was only found for *fgfr4* mutants, the lack of phenotypes in single *fgfr1a*, *fgfr1b*, *fgfr2*, *and fgfr3* mutants is likely due to genetic redundancy, not genetic compensation.

fgfr1a and fgfr1b are required for posterior mesoderm development

In vertebrates, the tail derives from the tailbud—a population of multipotent cells that forms at the caudal end of the embryo at the end of gastrulation. (Kimelman 2016). These cells undergo proliferation and differentiation, resulting in the elongation of the body axis in the posterior direction. Lineage analyses have shown that the tailbud gives rise to the posterior neural tube, notochord, and somites (Kanki and Ho 1997; Davis and Kirschner 2000). Fgf signaling is known to play a role in posterior mesoderm development; both *Fgfr1* and *Fgf8* mouse mutants lack posterior mesoderm due to failures in mesodermal specification and morphogenesis at the primitive streak (Deng *et al.* 1994; Yamaguchi *et al.* 1994; Sun *et al.* 1999; Ciruna and Rossant 2001). In zebrafish, animals expressing a dominant-negative Fgfr form no posterior mesoderm (Griffin *et al.* 1995), whereas animals deficient for both *fgf8a* and *fgf24* have a somewhat less severe reduction of posterior mesoderm (Draper *et al.* 2003). In this latter study, it was shown that *fgf8a* and *fgf24* are together required to maintain, but not initiate, the expression of *ta* (*ntl/brachyury homolog a*) and *tbx16* (*spt*), T-box transcription factor genes known to be required for mesodermal specification (Kimmel *et al.* 1989; Halpern *et al.* 1993; Conlon *et al.* 1996; Zhang *et al.* 1998; Amacher *et al.* 2002; Warga *et al.* 2013). These expression defects are visible ~80% epiboly (Draper *et al.* 2003)—a time at which only *fgfr1a* and *fgfr1b* are expressed highly at the margin of the gastrulating embryo where mesodermal precursors reside (Rohner *et al.* 2009; Ota *et al.* 2010). By contrast, during gastrulation, *fgfr2* and *fgfr3* have minimal expression in mesodermal precursors, and *fgfr4* expression appears to be restricted to cells that reside closer to the animal pole (Ota *et al.* 2010). These expression data therefore identify *fgfr1a* and *fgfr1b* as the likely candidate receptors involved in posterior mesoderm development.

Previously, Rohner *et al.* (2009) showed a variable posterior defect in animals homozygous for *fgfr1a(t3R05H)* that were also injected with MOs targeting *fgfr1b*, suggesting that

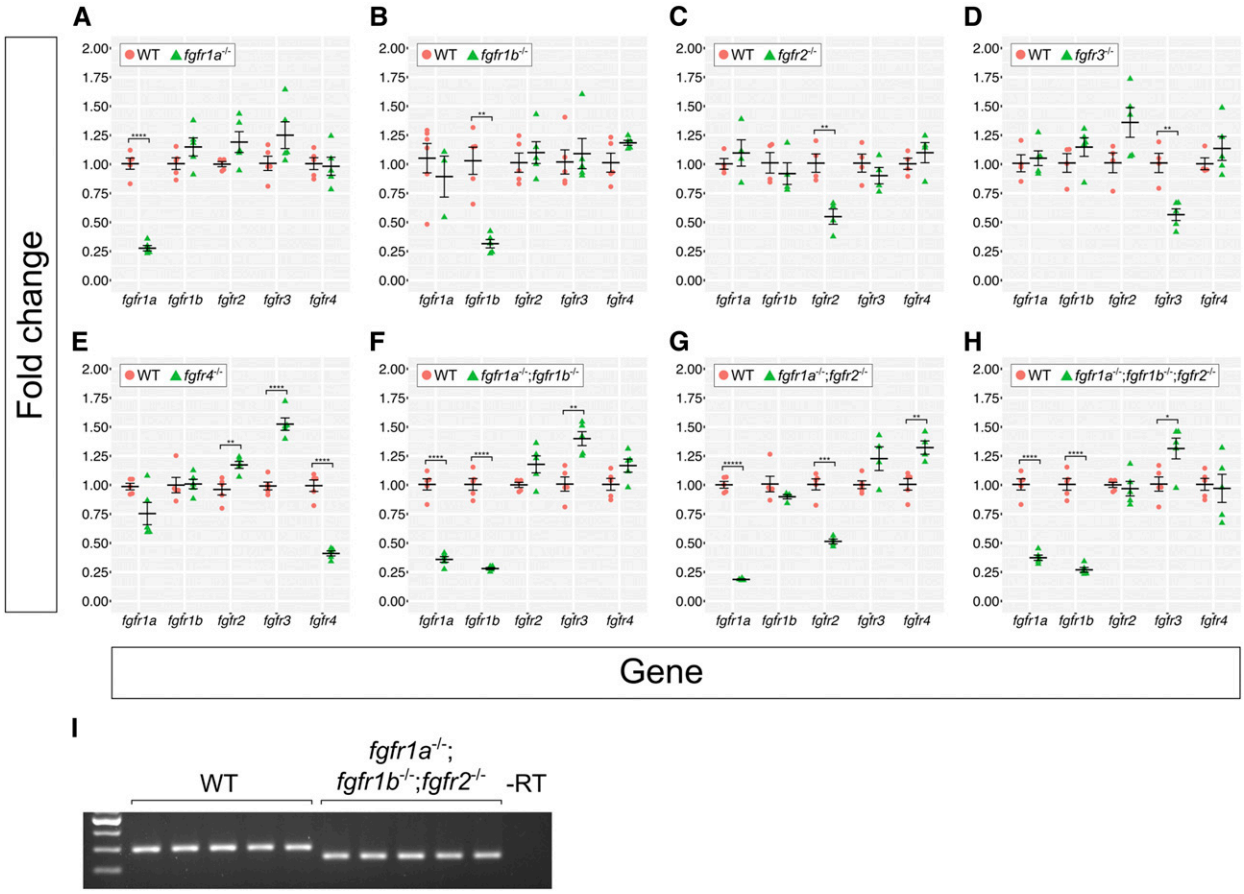

Figure 2 Fgf receptor mRNAs are overexpressed in some Fgf receptor mutants compared to wild-type embryos. (A–H) Fold changes calculated from RT-qPCR experiments comparing Fgf receptor mRNA levels between wild-type (WT, pink circles) and various Fgf receptor mutants (green triangles). Each point represents the mean fold change of an individual embryo, relative to WT. Error bars represent ± the SEM (center bar). Number of asterisks represents *P*-values calculated using a Student's *t*-test: no asterisk between WT and mutant denotes $P > 0.05$, $*P < 0.05$, $**P < 0.01$, $***P < 0.001$, $****P < 0.0001$, $*****P < 0.00001$. Results of the Student's *t*-test were confirmed using Multivariate ANOVA (MANOVA) tests (see *Materials and Methods*). (I) Because the *fgfr1a;fgfr1b;fgfr2* triple mutants represented in (H) displayed near-WT levels of *fgfr2* mRNA, *fgfr2* genotypes were confirmed with standard RT-PCR. Note the decreased band size in all *fgfr1a;fgfr1b;fgfr2* mutants.

these two receptor genes may play redundant roles in the formation of the posterior mesoderm. We therefore asked whether our *fgfr1a;fgfr1b* double mutant animals had defects in posterior mesoderm development. Although these double mutants die ~5 days postfertilization (dpf), we found that, in comparison to wild-type animals (Figure 3A), *fgfr1a;fgfr1b* double mutant animals have shorter and slightly kinked tails, and an accumulation of blood on the ventral side posterior to the yolk extension (Figure 3B). Because both *fgfr1a* and *fgfr1b* mRNAs are maternally provided (Figure 1B), it was possible that the mild defects observed were due to maternal gene product. To test this, we produced various combinations of maternal and/or zygotic loss of *fgfr1a* and *fgfr1b*. We found that Z*fgfr1*a;MZ*fgfr1b* mutants were largely indistinguishable from Z*fgfr1a*;Z*fgfr1b* mutants (Figure 3, B and C), arguing that maternally provided *fgfr1b* was not responsible for the mild phenotype. By contrast, we found that MZ*fgfr1a*;Z*fgfr1b* embryos had significantly shorter tails than Z*fgfr1a*;Z*fgfr1b* mutant embryos (Figure 3, B and D). These data argue that normal posterior mesoderm development requires zygotically expressed *fgfr1a* and *fgfr1b*, but also maternally expressed *fgfr1a*. Because *fgfr2* appears to be redundant with *fgfr1a* and *fgfr1b* in the other developmental contexts reported here (Figure 4, Figure 5, Figure 6, and Figure 7), we also asked whether the additional removal of functional *fgfr2* from Z*fgfr1a*;Z*fgfr1b* or MZ*fgfr1a*;Z*fgfr1b* double mutant embryos enhanced the respective phenotypes. However, these triple mutants underwent similar posterior mesoderm development to their double mutant counterparts, suggesting that *fgfr2* does not play a major role in this process (Figure S1, C and D).

To further examine the posterior defects, we compared gene expression between wild-type, Z*fgfr1a*;MZ*fgfr1b*, and MZ*fgfr1a*;Z*fgfr1b* 10-somite stage embryos by RNA *in situ* hybridization to assess the relative amounts of mesodermal derivatives produced. We costained embryos for the axial mesoderm marker *ta* (formerly *ntl*), which labels notochord cells (Schulte-Merker *et al.* 1992), and the paraxial mesodermal marker *myod*, which labels somitic mesoderm (Weinberg *et al.* 1996). We found that, while

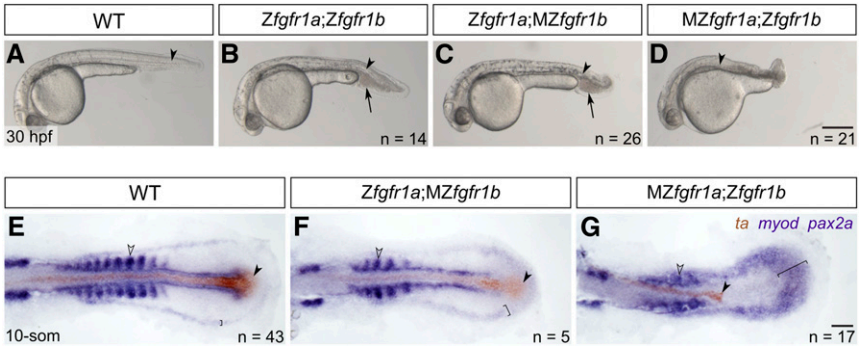

Figure 3 *fgfr1a* and *fgfr1b* function redundantly to regulate posterior mesoderm development. (A–D) Lateral view of 30 hpf wild-type (WT; A), and Z*fgfr1a*;Z*fgfr1b* (B), Z*fgfr1a*;MZ*fgfr1b* (C), and MZ*fgfr1a*;Z*fgfr1b* (D) mutant embryos. Arrowheads denote the notochord; arrows mark pooled blood cells in (B and C). Anterior is to the left, dorsal is up. (E–G) Mesodermal derivative marker analysis of Z*fgfr1a*;MZ*fgfr1b* and MZ*fgfr1a*;Z*fgfr1b* double mutant embryos at the 10-somite stage. The notochord (labeled with *ta*, brown; filled arrowhead) extends down the length of the trunk and tail in wild-type (E) and Z*fgfr1a*;MZ*fgfr1b* double mutant embryos (F), but is truncated in MZ*fgfr1a*;Z*fgfr1b* double mutant embryos (G). Defined somites (labeled with *myod*, purple; open arrowhead) are present in wild-type embryos (E) and Z*fgfr1a*;MZ*fgfr1b* embryos (F); however, the latter have distinctly fewer somites (5 compared to 10). Although MZ*fgfr1a*;Z*fgfr1b* mutants retain some *myod*-positive cells, there are no definitive somites (G). Pronephric precursors (labeled with *pax2a*, purple; brackets) are restricted to a defined band around the trunk and tail of wild-type embryos (E), a region that is expanded in both Z*fgfr1a*;MZ*fgfr1b* (F) and MZ*fgfr1a*;Z*fgfr1b* double mutant embryos (G). Bars: in (D), 200 μm for (A–D); in (G), 50 μm for (E–G).

wild-type and Z*fgfr1a*;MZ*fgfr1b* embryos have a notochord that extends down the entire length of the trunk and tail, MZ*fgfr1a*;Z*fgfr1b* mutant embryos formed notochord only in the trunk region (filled arrowheads, Figure 3, E–G). Similarly, we found that, at 14 hpf, when wild-type embryos had produced 10 somites, Z*fgfr1a*;MZ*fgfr1b* embryos have formed only 5 somites (Figure 3, E and F). Finally, in MZ*fgfr1a*; Z*fgfr1b* mutant embryos, although somitic mesoderm appears to have formed based on *myod* expression, proper somite morphogenesis appears to have failed (Figure 3G; open arrowhead). These findings are similar to that of *fgf8a* mutants injected with *fgf24* MOs, suggesting that these ligands signal, at least in part, via Fgfr1a and Fgfr1b during posterior mesoderm development. However, MZ*fgfr1a*;Z*fgfr1b* mutants form more posterior mesoderm than *fgf8a* mutant; *fgf24*MO animals (Draper *et al.* 2003), and significantly more than animals expressing a dominant-negative Fgfr (Griffin *et al.* 1995). We therefore hypothesize that residual activity of one or more of the remaining three Fgf receptors (Fgfr2, Fgfr3, Fgfr4) must be sufficient to promote partial production of posterior tissue.

pax2a is a marker of pronephric precursors, and, in wild-type embryos, is restricted to a discrete domain of lateral plate mesoderm in the 10-somite stage embryo (Krauss *et al.* 1991; Draper *et al.* 2003; bracket, Figure 3E). By contrast, Z*fgfr1a*;MZ*fgfr1b*, and, to a greater extent, MZ*fgfr1a*; Z*fgfr1b* mutants have an expanded region of *pax2a*-expressing cells, suggesting that these mutants produce an increased number of pronephric precursors relative to wild-type embryos (brackets, Figure 3, F and G). Additionally, Z*fgfr1a*; Z*fgfr1b* and Z*fgfr1a*;MZ*fgfr1b* mutants have an accumulation of blood cells just posterior to the yolk extension, similar to dorsalized mutants, such as *chordin* (Wagner and Mullins 2002; arrows, Figure 3, B and C). Given that the pronephros and blood are derived from lateral plate mesoderm, and somites and notochord arise from more dorsal paraxial and axial mesoderm, respectively, these data are consistent with previous analyses of *fgf8a* mutants, which concluded that Fgf signaling is important for promoting dorsal mesodermal fates (Furthauer *et al.* 1997, 2004; Schier and Talbot 2005).

fgfr1a, fgfr1b, and fgfr2 are required for pectoral fin development

Pectoral fins are the equivalent of mammalian forelimbs, and, with few exceptions, their development is regulated by orthologs of genes that regulate mammalian forelimb development (Mercader 2007). Studies using mouse, chick, and zebrafish have identified the important and conserved signaling ligands that participate in this process (Zuniga 2015; Figure 4A). For example, in both forelimb and pectoral fin development, the limb field within the lateral plate mesoderm (LPM) is specified by signals produced by the paraxial (retinoic acid) and intermediate (FGF8 and WNT2B) mesoderm, which initiates expression of the T-box transcription factor gene, *TBX5/tbx5a*, in the LPM (Cohn *et al.* 1995; Crossley *et al.* 1996b; Kawakami *et al.* 2001; Ng *et al.* 2002; Gibert *et al.* 2006). Subsequently, TBX5/Tbx5a activates the expression of an Fgf ligand, *Fgf10/fgf10a* within the LPM (Min *et al.* 1998; Ng *et al.* 2002). In zebrafish, this step is mediated by another Fgf ligand, Fgf24 (Min *et al.* 1998; Ng *et al.* 2002; Fischer *et al.* 2003). FGF10/Fgf10a in turn acts upon the overlying ectoderm to initiate formation of the apical ectodermal ridge (AER)—a structure that reciprocally signals back to the mesoderm via additional Fgf ligands (*e.g.*, FGF2, FGF4, FGF8 in mouse and chick; Fgf4, Fgf8a, Fgf24, and Fgf16 in zebrafish; Niswander and Martin 1992; Fallon *et al.* 1994; Laufer *et al.* 1994; Crossley *et al.* 1996b; Kengaku *et al.* 1998; Min *et al.* 1998; Kawakami *et al.* 2001; Sun *et al.* 2002; Fischer *et al.* 2003; Nomura *et al.* 2006) to maintain the expression of fin development genes within the fin bud mesenchyme. This Fgf-dependent feedback loop is maintained for the duration of limb development, and is required for limb outgrowth and patterning along the proximodistal axis (reviewed in Xu *et al.* 1999b). Thus, limb development requires a complex signaling network—of which Fgf signaling is a key component—to coordinate its development.

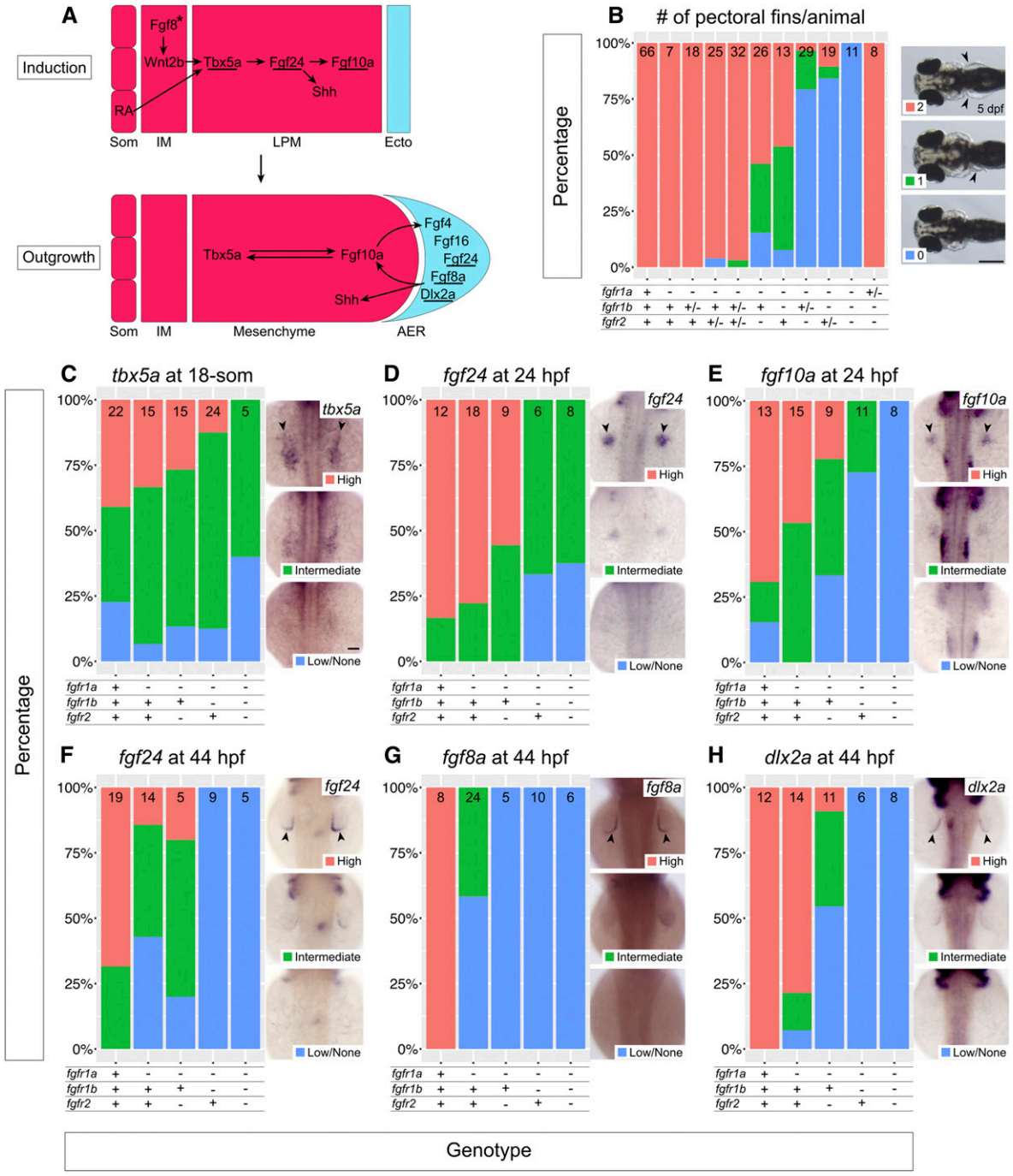

Figure 4 *fgfr1a*, *fgfr1b*, and *fgfr2* function redundantly to regulate pectoral fin development. (A) Model of pectoral fin bud development during pectoral fin bud Induction (top) and Outgrowth (bottom). Underlines denote genes assayed in (C–H). Arrows denote an epistatic (but not direct) link between molecules. Asterisk signifies that Fgf8 has not yet been shown to play this role in zebrafish, but is hypothesized from forelimb work in chick and mouse. (B) Stacked column chart depicting the average number of pectoral fins per animal at 5 dpf, according to genotype. Sample size for each genotype is listed at the top of each bar. Representative images of larvae with 2, 1, or 0 pectoral fins to the right: dorsal views, anterior to the left, with arrowheads denoting pectoral fins where present. (C–H) Fin bud marker analysis of *fgfr* double and triple mutant embryos at the 18-somite stage (*tbx5a*, C), 24 hpf (*fgf24*, D; *fgf10a*, E), and 44 hpf (*fgf24*, F; *fgf8a*, G; *dlx2a*, H). Whole mount *in situ* hybridization was performed, embryos were scored for expression, and genotypes were determined *post hoc*. In each panel, the percentage of embryos expressing particular levels of each marker gene is represented in a stacked column chart on the left, and representative images of those expression levels are shown for each marker to the right (dorsal views, anterior up; developing fin buds are seen as two spots on either side of the embryo, denoted by arrowheads). Bars: in (B), 200 μm; in (C), 50 μm for (C–H).

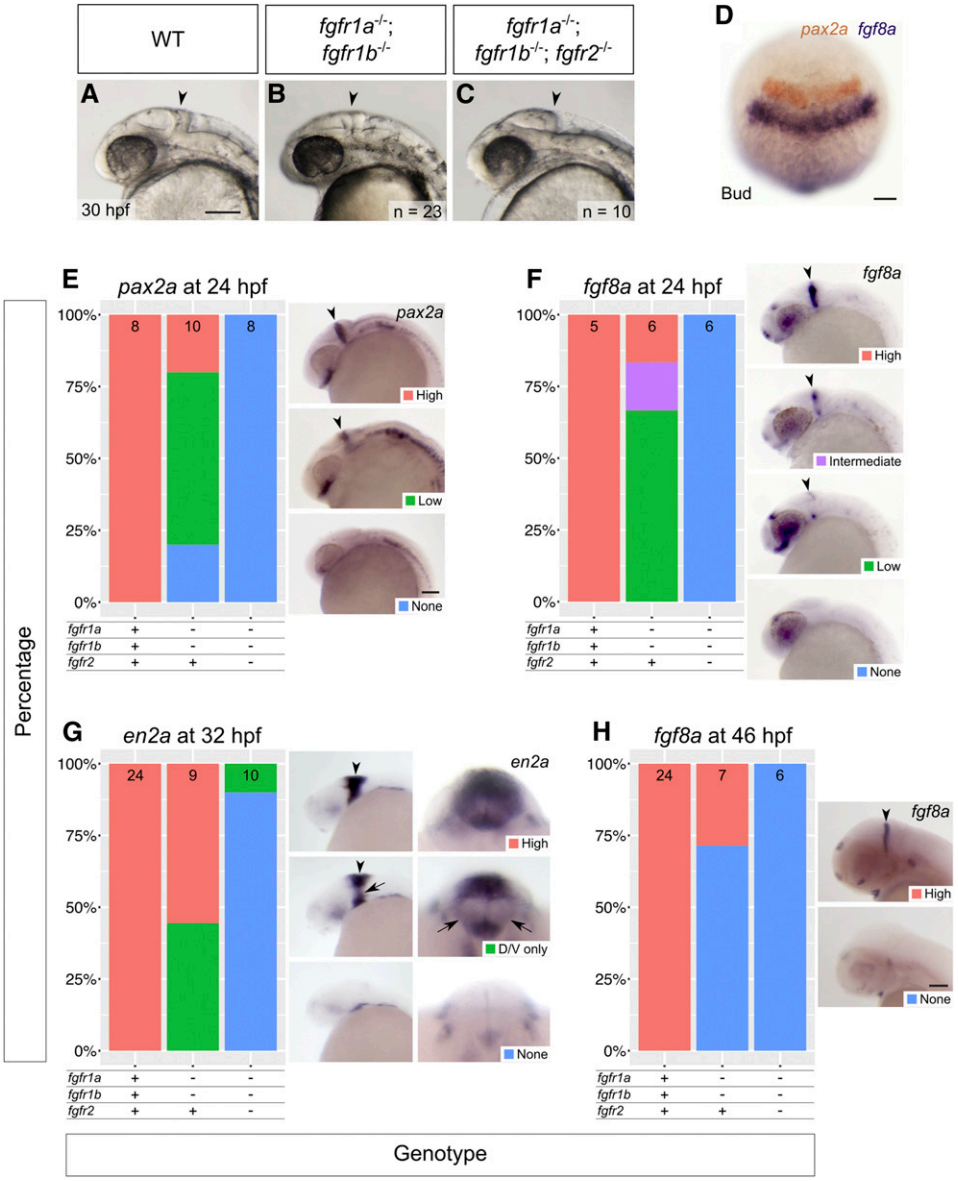

Figure 5 *fgfr1a*, *fgfr1b*, and *fgfr2* function redundantly to regulate MHB development. (A–C) Lateral view of 30 hpf wild-type (WT, A), and *fgfr1a*$^{-/-}$;*fgfr1b*$^{-/-}$ (B; n = 23), *fgfr1a*$^{-/-}$;*fgfr1b*$^{-/-}$;*fgfr2*$^{-/-}$ (C; n = 10) mutant embryos. Arrowheads denote region where the MHB should form. Rostral is to the left, dorsal is up. (D–H) MHB marker analysis of *fgfr* double and triple mutant embryos at the bud stage (*pax2a* in brown/*fgf8a* in purple, D), 24 hpf (*pax2a*, E; *fgf8a*, F), 32 hpf (*en2a*, G), and 46 hpf (*fgf8a*, H). Whole mount *in situ* hybridization was performed, embryos were scored for expression, and genotypes were determined *post hoc*. All embryos had indistinguishable *pax2a*/*fgf8a* expression at the bud stage (D; n = 28, 6, 4, for WT, *fgfr1a*$^{-/-}$;*fgfr1b*$^{-/-}$, and *fgfr1a*$^{-/-}$;*fgfr1b*$^{-/-}$;*fgfr2*$^{-/-}$, respectively). In (E–H), the percentage of embryos expressing particular levels of each marker gene is represented in a stacked column chart on the left (sample size for each genotype is listed at the top of each bar), and representative images of those expression levels are shown for each marker to the right (lateral views, rostral to the left and dorsal up; developing MHBs are denoted by arrowheads). Rightmost images in (G) are magnified frontal views (dorsal up) showing low *en2a* staining in the left and right regions of the cerebellum (arrows). Bars: in (A), 100 μm for (A–C); in (D), 100 μm; in (E), 100 μm for (E–G); in (H), 100 μm.

In mouse, null mutations of *Fgfr1* and *Fgfr2* result in embryonic lethality before the end of gastrulation, precluding their use for determining their role in limb development (Deng *et al.* 1994; Yamaguchi *et al.* 1994; Arman *et al.* 1998). However, the use of hypomorphic alleles has led to the conclusion that FGFR1 is involved in limb patterning, while FGFR2 has a more prominent role in limb bud induction and outgrowth (Xu *et al.* 1998, 1999a,b; De Moerlooze *et al.* 2000). Given these findings, and the established roles for Fgf ligands throughout limb development, it was surprising that all five single *fgfr* mutants have normal pectoral fin development (arrowheads, Figure 4B, and data not shown). However, *fgfr1a*, *fgfr1b*, and *fgfr2* are all expressed in the developing fin bud (Thisse and Thisse 2005; Harvey and Logan 2006; Thisse *et al.* 2008; Camarata *et al.* 2010; Rohs *et al.* 2013), suggesting that these receptors may play redundant roles in fin development. Consistent with this hypothesis, at 5 dpf we found that 54% of *fgfr1a*$^{-/-}$;*fgfr1b*$^{-/-}$ double mutants, and 46% of *fgfr1a*$^{-/-}$;*fgfr2*$^{-/-}$ double mutants, lack at least one pectoral fin (n = 13 and n = 26, respectively), establishing a role for all three of these receptors in pectoral fin development. Removing the function of an additional *fgfr* allele in these double homozygous mutants increases the penetrance of the pectoral fin phenotype: 90% of *fgfr1a*$^{-/-}$;*fgfr1b*$^{-/-}$;*fgfr2*$^{+/-}$ and 97% of *fgfr1a*$^{-/-}$;*fgfr1b*$^{+/-}$;*fgfr2*$^{-/-}$ lack at least one pectoral fin (n = 19 and n = 29, respectively). Finally, 100% of *fgfr1a*$^{-/-}$;*fgfr1b*$^{-/-}$;*fgfr2*$^{-/-}$ triple mutants fail to form any pectoral fins (n = 11; Figure 4B), indicating that these three receptors act redundantly to promote zebrafish pectoral fin development. Interestingly, the presence of a single wild-type copy of *fgfr1a* is sufficient to rescue this phenotype completely (Figure 4B), suggesting that *fgfr1a* is particularly important for pectoral fin development.

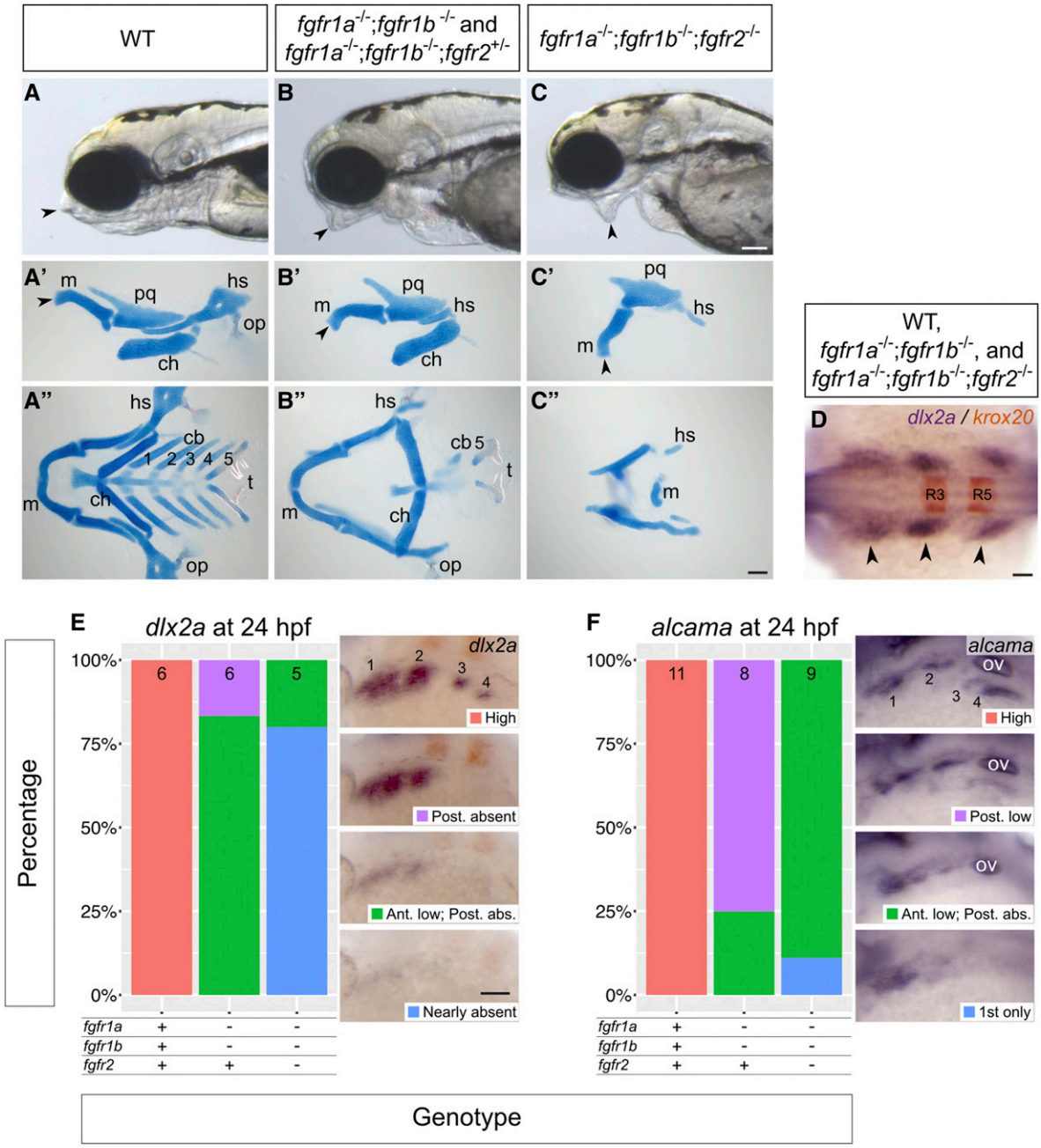

Figure 6 *fgfr1a*, *fgfr1b*, and *fgfr2* function redundantly to regulate viscerocranial development. (A–C) Lateral views of 5 dpf wild-type (WT, A; *n* = 12), *fgfr1a*$^{-/-}$;*fgfr1b*$^{-/-}$ (*n* = 3)/*fgfr1a*$^{-/-}$;*fgfr1b*$^{-/-}$;*fgfr2*$^{+/-}$ (B; *n* = 6), *fgfr1a*$^{-/-}$;*fgfr1b*$^{-/-}$;*fgfr2*$^{-/-}$ (C; *n* = 7) mutant larvae. (A′–C′′) Alcian blue cartilage stains of 5 dpf larvae; arrowheads noting corresponding jaw features between the live larvae in (A–C) and lateral view cartilage mounts in (A′–C ′); m, Meckel's cartilage; pq, palatoquadrate; hs, hyosymplectic; ch, ceratohyal; op, operculum; cb 1–5, ceratobranchials; t, teeth. (D–F) Pharyngeal arch (D and E) and pouch (F) marker analysis of *fgfr* double and triple mutant embryos at the 18-somite stage (*dlx2a* in purple/*krox20* in brown labeling rhombomeres 3 (R3) and 5 (R5); D) and 24 hpf (*dlx2a*, E; *alcama*; F). Whole mount *in situ* hybridization was performed, embryos were scored for expression, and genotypes were determined *post hoc*. All embryos had indistinguishable *dlx2a* expression at the 18-somite stage (D; *n* = 7, 26, 6, for WT, *fgfr1a*$^{-/-}$;*fgfr1b*$^{-/-}$, and *fgfr1a*$^{-/-}$;*fgfr1b*$^{-/-}$;*fgfr2*$^{-/-}$, respectively). In (E and F), the percentage of embryos expressing particular levels of each marker gene is represented in a stacked column chart on the left (sample size for each genotype is listed at the top of each bar), and representative images of those expression levels are shown for each marker to the right (dorsolateral views, rostral to the left and dorsal up; pharyngeal arches (E) and pouches (F) are labeled 1–4. Bars: in (C), 100 μm for (A–C); in (C′′), 100 μm for (A′–C′′); in (D), 50 μm; in (E), 100 μm for (E and F). abs., absent; Ant., Anterior arches/pouches; in (F), ov, otic vesicle; Post., Posterior arches/pouches.

In zebrafish, pectoral fin bud initiation occurs around the 18-somite stage (18 hpf), as evident by the expression of *tbx5a*, one of two orthologs of mouse and chick *Tbx5* (Ahn *et al.* 2002; Garrity *et al.* 2002; Ng *et al.* 2002). Shortly thereafter, Tbx5a promotes the transcription of *fgf24* within the fin bud mesoderm, which is then required for mesodermal

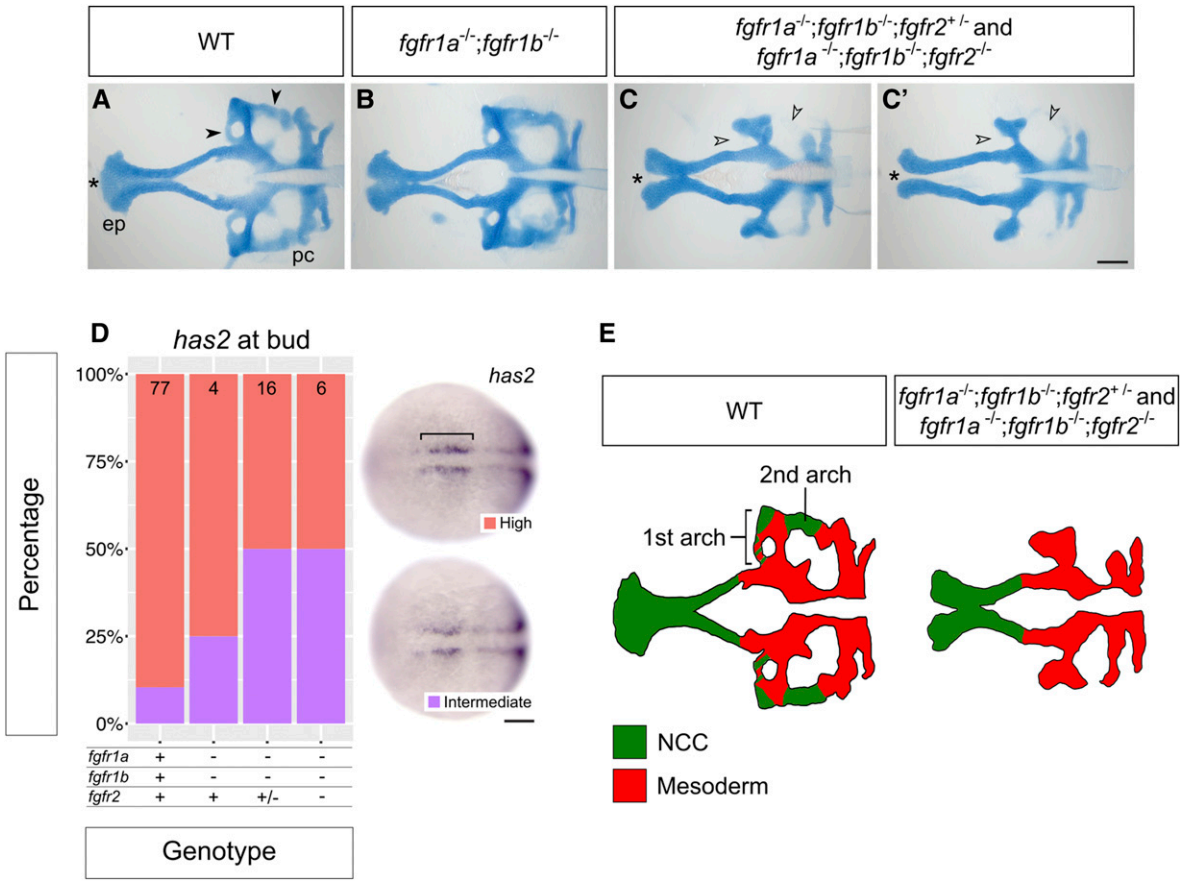

Figure 7 *fgfr1a*, *fgfr1b*, and *fgfr2* function redundantly to regulate neurocranial development. (A–C′) Alcian blue cartilage staining of 5 dpf wild-type (WT, A; n = 12), $fgfr1a^{-/-};fgfr1b^{-/-}$ (B; n = 3), $fgfr1a^{-/-};fgfr1b^{-/-};fgfr2^{+/-}$ (n = 6)/$fgfr1a^{-/-};fgfr1b^{-/-};fgfr2^{-/-}$ (n = 7) (C and C′) mutant larvae. Notice the variable fusion of the trabeculae (*) in $fgfr1a^{-/-};fgfr1b^{-/-};fgfr2^{-/-}$ triple mutants (C and C′) compared to WT (A); full fusion in 3/7 animals, partial fusion in 2/7 animals, no fusion in 2/7 animals. Open arrowheads in (C and C′) denote missing regions of the postchordal neurocranium [compare filled arrowheads in (A)]. (D) Cephalic mesoderm marker analysis of *fgfr* double and triple mutant embryos at the bud stage using *has2*. Whole mount *in situ* hybridization was performed, embryos were scored for expression, and genotypes were determined *post hoc*. The percentage of embryos expressing "High" or "Intermediate" *has2* expression is represented in a stacked column chart on the left (sample size for each genotype is listed at the top of each bar), and representative images of those expression levels are shown for each marker to the right (dorsal views, rostral to the left; bracket denotes cells specified for cephalic development. (E) Traces of cartilage mounts in (A and C), filled in with expected lineage contributions, adapted with permission from McCarthy *et al.* (2016). Bars: in (C), 100 μm for (A–C′); in (D), 50 μm. ep, ethmoid plate; pc, postchordal neurocranium.

transcription of *fgf10a* and *sonic hedgehog* (*shh*; involved in anterior-posterior patterning of fins and limbs) (Krauss *et al.* 1991, 1993; Neumann *et al.* 1999; Ng *et al.* 2002; Fischer *et al.* 2003). Fgf10a maintains *tbx5a* expression in the fin bud mesoderm, and is likely responsible for signaling to the overlying ectoderm to induce AER formation, which includes the induction of *fgf8a*, *fgf4*, *fgf24*, and *fgf16* expression in the ectoderm by ~30–36 hpf (Reifers *et al.* 1998; Grandel *et al.* 2000; Ng *et al.* 2002; Fischer *et al.* 2003; Nomura *et al.* 2006). In chick and mouse, this induction appears to be mediated by WNT signaling (Kengaku *et al.* 1998; Kawakami *et al.* 2001); however, this has yet to be established in zebrafish. Similar to chick and mouse, it is likely that the AER Fgfs signal back to the fin bud mesenchyme to stabilize *fgf10a* expression, thus establishing a positive regulatory feedback loop required for fin bud outgrowth (Camarata *et al.* 2010; Figure 4A).

Because Fgf signaling is known to mediate many tissue interactions during limb and fin development, we sought to characterize at what level the various mutant combinations affect fin development by assessing the expression of marker genes using RNA *in situ* hybridization at different stages of fin bud development. Following *in situ* hybridization, embryos were scored for marker gene expression first and then genotyped. We initially asked if any of the mutant combinations affected fin bud initiation by assaying the expression of *tbx5a*—the earliest marker of pectoral fin bud induction (Ahn *et al.* 2002). In wild-type embryos, *tbx5a* expression in the LPM could be detected in most, but not all, 18-somite stage embryos—a stage that precedes feedback regulation from the LPM expressed Fgfs (Figure 4, A and C). Expression was similarly detected in all other genotypes examined, including $fgfr1a^{-/-};fgfr1b^{-/-};fgfr2^{-/-}$ triple mutants, though the triple mutants had, on average, less intense staining (Figure 4C). These results suggest that the first steps of fin bud induction are only mildly affected by loss of Fgfr1a, Fgfr1b, and Fgfr2 functions (Figure 4C).

In zebrafish, Tbx5a induces the expression of *fgf24* in the LPM, and Fgf24 signals within the LPM to stimulate *fgf10a* expression, which, in turn, is thought to form a feedback loop to maintain *tbx5a* expression (Ng *et al.* 2002; Fischer *et al.* 2003; Figure 4A). While the expression of *fgf24* and *fgf10a* is easy to detect by *in situ* hybridization in most 24 hpf wild-type fin buds, their expression is reduced or not detected in 24 hpf *fgfr1a;fgfr1b* and *fgfr1a;fgfr2* double mutant and *fgfr1a;fgfr1b;fgfr2* triple mutant fin buds (Figure 4, D and E). These results suggest that, although the fin bud is induced in these mutants, Fgfr1a, Fgfr1b, and Fgfr2 are redundantly required to maintain gene expression within the fin bud mesenchyme.

During the outgrowth phase of fin development (24 – ~48 hpf; Grandel and Schulte-Merker 1998), Fgfs from the fin bud mesenchyme signal the ectoderm to form the AER. We therefore asked if AER-specific gene expression was reduced in *fgfr1a;fgfr1b* and *fgfr1a;fgfr2* double mutants and *fgfr1a;fgfr1b;fgfr2* triple mutants. Indeed, whereas *fgf24*, *fgf8a*, and *dlx2a* are all expressed in the AER of wild-type animals at 44 hpf, the number of embryos with reduced or no detectable expression by *in situ* hybridization is greatly increased in the various mutant combinations (Figure 4, F–H). Interestingly, in *fgfr1a* single-mutant embryos, which have normal pectoral fin development, we also observed a reduction in AER-expressed *fgf24* and *fgf8a* at 44 hpf (Figure 4, F and G). Together, these results suggest that Fgfr1a, Fgfr1b, and Fgfr2 function redundantly to maintain proper gene expression in the fin bud mesenchyme, and, subsequently, in the AER, but that *fgfr1a* may be particularly important at the mesenchyme/AER interface. This may explain why the presence of a single wild-type copy of *fgfr1a* is sufficient to rescue the *fgfr1a;fgfr1b;fgfr2* triple mutant pectoral fin phenotype (Figure 4B).

fgfr1a, fgfr1b, and fgfr2 are required for brain development

The vertebrate brain develops from the relatively simple neural plate. One of the earliest patterning events of the neural plate is its subdivision into rostral and caudal domains that can be identified by expression of the transcription factors *Otx2* and *Gbx2*, respectively (Broccoli *et al.* 1999; Millet *et al.* 1999). A signaling center called the midbrain-hindbrain organizer forms at the boundary of these domains, which acts to pattern the surrounding neural tissues (Marin and Puelles 1994; Martínez *et al.* 1995). Fgf signaling is the most prominent signaling pathway in the MHB, and, while many Fgf ligands are known to be expressed in the MHB organizer (Fgf8, Fgf17, Fgf18, Fgf4), Fgf8 appears to have the most critical role: in chick, FGF8-soaked beads ectopically induce midbrain development (Crossley *et al.* 1996a), whereas mutations in mouse *Fgf8*, or its ortholog *fgf8a* in zebrafish, result in loss of the MHB and cerebellum (Brand *et al.* 1996; Meyers *et al.* 1998; Reifers *et al.* 1998; Chi *et al.* 2003).

In mouse, tissue-specific knockout of *Fgfr1* in MHB cells, or an *Fgfr1* hypomorphic mutation, leads to the loss of certain MHB structures (Trokovic *et al.* 2003). However, this phenotype is less severe than that of *Fgf8* mutants, suggesting that other receptors are involved in FGF8 signal transduction during MHB development (Chi *et al.* 2003; Trokovic *et al.* 2003). In zebrafish, *fgfr1a* is expressed at high levels in the developing MHB region (Tonou-Fujimori *et al.* 2002; Scholpp *et al.* 2004; Rohner *et al.* 2009; Ota *et al.* 2010; Larbuisson *et al.* 2013; Rohs *et al.* 2013; Koch *et al.* 2014) and MO knockdown of *fgfr1a* has been reported to phenocopy *fgf8a* mutants (Scholpp *et al.* 2004). By contrast to the *fgfr1a* morphants, *fgfr1a(uc61)* (Figure 1D) and *fgfr1a(t3R05H)* (Rohner *et al.* 2009) mutants have normal MHB development, arguing that, in zebrafish, Fgf receptors in addition to Fgfr1a are able to mediate Fgf8a signaling during MHB development.

Zebrafish *fgf8a* mutants first display gene expression abnormalities in the hindbrain region during early somitogenesis, with increasing severity by late somitogenesis (18-somite stage) (Reifers *et al.* 1998). At the 18-somite (18 hpf) and Prim-5 (24 hpf) stages, when the MHB signaling center is active, *fgfr1a*, *fgfr1b*, and *fgfr2* are expressed in, or immediately adjacent to, the MHB (Thisse *et al.* 2001, 2008; Tonou-Fujimori *et al.* 2002; Scholpp *et al.* 2004; Thisse and Thisse 2005; Rohner *et al.* 2009; Ota *et al.* 2010; Larbuisson *et al.* 2013; Rohs *et al.* 2013; Koch *et al.* 2014; Lovely *et al.* 2016). Considering the apparent role for FGFR1 in maintenance of midbrain and hindbrain tissue in the mouse, we first tested if *fgfr1a;fgfr1b* double mutants would lead to a brain defect similar to that of the *fgf8a* mutation. However, the MHBs of these animals are morphologically indistinguishable from wild type (arrowheads, Figure 5, A and B). In contrast, the triple mutant *fgfr1a;fgfr1b;fgfr2* appears to phenocopy the acerebellar phenotype of *fgf8*a mutants (arrowhead, Figure 5C).

To further assess the brain development of these animals, we used RNA *in situ* hybridization to assay the expression of genes known to play a role in MHB development. At the bud stage of development (10 hpf), *pax2a* and *fgf8a* label the prospective MHB (Krauss *et al.* 1991; Mikkola *et al.* 1992; Reifers *et al.* 1998). In all genotypes examined, including *fgfr1a;fgfr1b;fgfr2* triple mutants, we found that both genes are expressed in their stereotypic locations, suggesting that the specification of MHB cells is unaffected (Figure 5D). In contrast, at 24 hpf, when both *pax2a* and *fgf8a* are still expressed in the MHB of wild-type embryos, their expression is not detected in the MHB of *fgfr1a;fgfr1b;fgfr2* triple mutants (Figure 5, E and F). Consistently, the cerebellar marker *en2a* is absent from most triple mutants by 32 hpf (Millen *et al.* 1994; Figure 5, G and H).

Although the induction of prospective MHB genes and MHB morphology is normal in *fgfr1a;fgfr1b* double mutants (Figure 5, B and D), we found that marker gene expression was reduced in many double mutant embryos when compared to wild-type animals at 24 hpf, and, by 46 hpf, *fgf8a* expression is not detectable in ~70% of double mutant embryos (Figure 5, E–H). These data suggest that a partial reduction in Fgf signaling is sufficient to affect gene expression

in the MHB, but not overt MHB morphology. Though it is possible that brain patterning, and therefore brain function, is compromised in these animals, we have not been able to test this prospect, as they do not survive past 5 dpf.

fgfr1a, fgfr1b, and fgfr2 are required for craniofacial skeletal development

Skeletal structures of the head are largely derived from cranial neural crest cells. During development, neural crest cells (NCCs) migrate ventrolaterally from the dorsal neuroectoderm of the hindbrain into endodermal pockets called pharyngeal pouches. There, intrinsic cues and inductive signaling from the surrounding tissue instruct NCC development into cartilage (reviewed in Kimmel *et al.* 2001; Mork and Crump 2015). In zebrafish, seven arches form between the endodermally derived pouches, and most arch derivatives compose the viscerocranium: the first arch gives rise to Meckel's cartilage and the palatoquadrate; the second gives rise to the ceratohyal and hyosemplectic; and arches three to seven give rise to the ceratobranchials (Schilling and Kimmel 1994; Kimmel *et al.* 2001; Crump *et al.* 2004b, 2006). However, lineage tracing has revealed that NCCs also give rise to the neurocranium; NCCs from the first two arches contribute to discrete portions of the postchordal neurocranium, whereas the prechordal neurocranium arises from more anteriorly derived NCCs (Wada *et al.* 2005; Eberhart *et al.* 2006; Swartz *et al.* 2011; McCarthy *et al.* 2016).

Many Fgfs and their receptors are expressed throughout the head during the time of cranial cell specification and differentiation (Scholpp *et al.* 2004; Nechiporuk *et al.* 2005; Rohner *et al.* 2009; Ota *et al.* 2010; Larbuisson *et al.* 2013; Rohs *et al.* 2013), and several of the processes underlying cranial morphogenesis are known to be driven by Fgf signaling. In mouse, *Fgf8* is required for proper development of several pharyngeal arch-derived craniofacial structures, and FGFR1 and FGFR2 play an important role in mammalian palatogenesis (Abu-Issa *et al.* 2002; Rice *et al.* 2004; Yu *et al.* 2015). In zebrafish, *fgf8a;fgf3* double mutants do not form the posterior viscerocranium, have severely deformed anterior viscerocranium, and do not form the mesodermally derived cartilages of the postchordal neurocranium (Crump *et al.* 2004a; McCarthy *et al.* 2016). Furthermore, MO analysis suggests that the Fgf receptors Fgfr1a and Fgfr2 can each regulate late cartilage formation in the viscerocranium, although the effects are attributed to later defects compared to those caused by loss of *fgf8a* and *fgf3* (Larbuisson *et al.* 2013). However, we found that cranial development in *fgfr1a* and *fgfr2* single mutants, as well as *fgfr1a*; *fgfr2* double mutants were indistinguishable from wild type (data not shown). By contrast, we found that *fgfr1a;fgfr1b* double mutants have reduced viscerocrania, including a loss of most of the ceratobranchials and hyosymplectic, and also have misshapen palatoquadrate and Meckel's cartilage (Figure 6, B–B′′). Although *fgfr1a;fgfr1b* double mutant animals that are also heterozygous for a null allele of *fgfr2* (*i.e.*, *fgfr1a*$^{-/-}$*;fgfr1b*$^{-/-}$*;fgfr2*$^{+/-}$) are indistinguishable from *fgfr1a*$^{-/-}$*;fgfr1b*$^{-/-}$*;fgfr2*$^{+/+}$ animals with respect to viscerocrania development (Figure 6, B–B′′), both *fgfr1a*$^{-/-}$*;fgfr1b*$^{-/-}$*;fgfr2*$^{+/-}$ and *fgfr1a*$^{-/-}$*;fgfr1b*$^{-/-}$*;fgfr2*$^{-/-}$ mutants lack portions of the postchordal neurocranium that are thought to be derived from the first and second pharyngeal arches (Figure 7, C and C′). Finally, of all genotypes analyzed, *fgfr1a;fgfr1b;fgfr2* triple mutants have the most severe cranial defects: in addition to an abnormal postchordal neurocranium (Figure 7, C and C′), the viscerocranial ceratobranchials, ceratohyal, and most of the hyosymplectic fail to form, the palatoquadrate is misshapen, and Meckel's cartilage is displaced downward (Figure 6, C–C′′). Together, these data suggest that Fgfr1a, Fgfr1b, and Fgfr2 function together to promote cranial cartilage formation.

Recent studies have proposed that, during development of the head skeleton, Fgf signaling is required either during pharyngeal pouch/arch formation or maintenance (Crump *et al.* 2004a), or later during cartilage formation (Larbuisson *et al.* 2013). We therefore asked at which stage our Fgfr mutations affect cranial development by assessing the expression of known marker genes of pharyngeal endoderm and NCCs—the cells that primarily form the pharyngeal pouches and arches, respectively. In a wild-type 18-somite stage embryo, NCCs expressing *dlx2a* have migrated into the pouches, where they form three distinct clusters on each side of the embryo, at the anterioposterior level of the midbrain and hindbrain (arrowheads, Figure 6D). The most anterior of these clusters will give rise to the first pharyngeal arch, the middle to the second arch, and the most posterior will later separate to give rise to arches three to seven. We found that embryos of all genotypes, including *fgfr1a;fgfr1b;fgfr2* triple mutants, have normal *dlx2a* expression at the 18-somite stage, indicating that NCCs successfully migrate to, and populate, the pharyngeal pouches (Figure 6D).

In a wild-type 24 hpf embryo (Prim-5 stage), the most posterior cluster of NCCs has begun to separate into two distinct domains (labeled 3 and 4 in Figure 6E), and *alcama*-labeled pharyngeal endoderm, which separates the arches, also separates into two domains posteriorly (labeled 3 and 4 in Figure 6F). In all 24 hpf *fgfr1a;fgfr1b* double- and *fgfr1a;fgfr1b;fgfr2* triple-mutant embryos, however, *dlx2a* and *alcama* expression is either reduced or not detected, with the largest reduction seen in the posterior-most arches and pouches, respectively (Figure 6, E and F). Together, these data suggest that NCC migration into the pharyngeal pouches occurs normally in mutants, but that these cells are not maintained. These data therefore argue for an early role of Fgf signaling in cranial development similar to that previously proposed by Crump *et al.* (2004a).

Previous fate-mapping experiments in zebrafish indicate that discrete regions of the postchordal neurocranium derive from both mesoderm and NCC (McCarthy *et al.* 2016; Figure 7E). Fgf8a and Fgf3 function redundantly to establish the mesodermal precursors that will make up this tissue, and embryos deficient for both ligands exhibit severely reduce

postchordal neurocranium (McCarthy *et al.* 2016). By contrast, the portions of cartilage missing from *fgfr1a*$^{-/-}$;*fgfr1b*$^{-/-}$;*fgfr2*$^{+/-}$ and *fgfr1a*$^{-/-}$;*fgfr1b*$^{-/-}$;*fgfr2*$^{-/-}$ mutant neurocrania appear to correspond solely with the NCC-derived regions of wild-type neurocrania (arrowheads, Figure 7, A, C, and D), while the mesodermally derived regions are retained. To confirm that mesodermal precursors are in fact preserved in *fgfr1a*$^{-/-}$;*fgfr1b*$^{-/-}$;*fgfr2*$^{+/-}$ and *fgfr1a*$^{-/-}$;*fgfr1b*$^{-/-}$;*fgfr2*$^{-/-}$ mutants, we used *in situ* hybridization to assess the expression of *has2*, which, in wild-type bud-stage embryos, is expressed in cephalic mesoderm precursor cells that localize to discrete bilateral domains flanking the anterior midline (Camenisch *et al.* 2000; McCarthy *et al.* 2016; bracket in Figure 7D). Unlike embryos deficient for both *fgf8a* and *fgf3*, which have reduced or no detectable expression of *has2* (McCarthy *et al.* 2016), we found little to no detectable difference in the expression of *has2* between wild type and *fgf* receptor mutants (Figure 7D). These results suggest that loss of Fgfr1a, Fgfr1b, and Fgfr2 functions does not affect the initial formation of the cephalic mesoderm, but is instead required for NCC maintenance in this tissue, similar to what we found for the NCCs during viscerocranial development (Figure 6, D–F).

Conclusions

The Fgf signaling pathway regulates numerous developmentally important processes. Although the identity of the specific Fgf ligand(s) that regulates these processes is known in many cases, less is known about the identity of the receptors that mediate particular cellular interactions. Here, we have described the generation and initial characterization of mutations in each of the five zebrafish Fgf receptor genes. We showed that all single mutants are viable and fertile as adults, but that double and triple mutant combinations have defects similar to those of known ligand mutants. These mutants have allowed us to genetically identify for the first time, or to confirm previous studies using MO oligo-based analysis, which receptors likely transduce the signaling of select ligands. One surprise is that all phenotypes described here require loss of Fgfr1a function, suggesting that this receptor is of prime importance for Fgf-dependent processes in early development. It is interesting that Fgfr1a is also the predominant maternally supplied receptor, and, as such, is likely uniformly translated in all cells during early development.

In most cases, estimating relevant receptor–ligand selectivity has relied on *in vitro* mitogenic assays, where ligands are tested for their ability to induce the proliferation of cells expressing a particular receptor or receptor isoform (Ornitz *et al.* 1996; Zhang *et al.* 2006). By contrast, probable receptor–ligand interactions investigated by *in vivo* mutational analysis have been limited, in part due to the lethal effect of introducing null mutations of *Fgfr1* or *Fgfr2* into the mouse genome (Deng *et al.* 1994; Yamaguchi *et al.* 1994; Arman *et al.* 1998). Our *in vivo* analysis suggests that there is not a one-to-one relationship, where each ligand stimulates a single receptor type, but that each ligand appears capable of interacting with multiple receptors. It remains to be seen if these ligands bind only to receptor homodimers, or if ligand binding is able to induce heterodimerization between different receptors that are expressed in the same cell.

Genetic redundancy or transcriptional compensation?

We anticipated that we would find genetic redundancy between *fgfr1a* and *fgfr1b*, as these ohnologs arose from a more recent genome duplication event than the more ancient event that gave rise to the other receptor orthologs (Rohner *et al.* 2009). The apparent genetic redundancy between the *fgfr* genes was especially striking in light of previous reports that MO knockdown of single *fgfr* genes can result in morphological abnormalities. For example, MOs that block translation or splicing of *fgfr1a* were shown to cause deformation of the MHB and pharyngeal cartilages (Scholpp *et al.* 2004; Larbuisson *et al.* 2013). Likewise, MO knockdown of *fgfr2* was reported to cause viscerocranial cartilage and left/right asymmetry defects (Liu *et al.* 2011; Larbuisson *et al.* 2013). It is possible that the MO gene knockdowns do not represent the true receptor loss-of-function phenotypes. Alternatively, it is possible that transcriptional adaptation, which can be induced by indel mutations that cause premature termination codons that triggers NMD of mutant mRNAs, is lessening the phenotypic severity of our indel mutations (Rossi *et al.* 2015; El-Brolosy *et al.* 2019; Ma *et al.* 2019). However, with the exception of *fgfr4* mutants, we do not detect significant changes in wild-type *fgfr* mRNA expression in our *fgfr* single mutants, suggesting that the lack of phenotype in these animals is likely due to redundancy, not genetic compensation (Figure 2, A–H). This notion is supported by previous studies showing that the expression domains of *fgfr1a*, *fgfr1b*, and *fgfr2* overlap extensively throughout the developing embryo, including in each of the tissues discussed here (Sleptsova-Friedrich *et al.* 2001; Thisse *et al.* 2001, 2008; Tonou-Fujimori *et al.* 2002; Scholpp *et al.* 2004; Nechiporuk *et al.* 2005; Thisse and Thisse 2005; Harvey and Logan 2006; Rohner *et al.* 2009; Camarata *et al.* 2010; Ota *et al.* 2010; Larbuisson *et al.* 2013; Rohs *et al.* 2013; Koch *et al.* 2014; Lovely *et al.* 2016). With regard to our double and triple mutant analysis, we detected a significant increase in wild-type *fgfr3* and *fgfr4* mRNAs, raising the possibility that the phenotypes we describe for these mutant combinations could be less severe than those caused by alleles that do not induce genetic compensation. Regardless, these mutant alleles have clearly allowed us to identify Fgf receptors that function in specific developmental processes, and to pair these receptors with their probable Fgf ligand(s).

We have shown several developmental processes that appear to use multiple Fgf receptors. This is not unique to zebrafish, as receptor redundancy has also been reported in mammals. For example, during lung development in mice, *Fgfr3*$^{-/-}$;*Fgfr4*$^{-/-}$ double mutants exhibit disrupted alveogenesis, whereas the lungs of single mutants are normal (Weinstein *et al.* 1998). Additionally, Zhao and colleagues

used conditional knockout of *Fgfr1* and *Fgfr2* in concert with *Fgfr3* mutation to show that these three receptors act redundantly during mouse lens development (Zhao *et al.* 2008). It is possible that this type of redundancy exists elsewhere in the mouse as well, but the early embryonic lethality of *Fgfr1* and *Fgfr2* mutations makes this a difficult area of study. Going forward, the zebrafish is an attractive model to investigate these questions, in the context of Fgf signaling.

Acknowledgments

We thank Kira Lin and Lan-Uyen Nguyen for assistance identifying and maintaining the alleles used in this report. We are grateful to members of the Draper, C. Erickson, P. Armstrong, L. Jao, S. Burgess, and C. Juliano laboratories (UC Davis) for valuable discussion of this work, and to Carol Erickson, Matt McFaul, and Sydney Wyatt for their critical review of this manuscript. This work was supported by the National Institute of Child Health and Development (1R01 HD081551-01A1) to B.W.D. and by the National Institute of General Medical Science (2 T32 GM007377) to D.M.L. The authors declare no competing interests.

Literature Cited

Abu-Issa, R., G. Smyth, I. Smoak, K. Yamamura, and E. N. Meyers, 2002 Fgf8 is required for pharyngeal arch and cardiovascular development in the mouse. Development 129: 4613–4625.

Ahn, D. G., M. J. Kourakis, L. A. Rohde, L. M. Silver, and R. K. Ho, 2002 T-box gene tbx5 is essential for formation of the pectoral limb bud. Nature 417: 754–758. https://doi.org/10.1038/nature00814

Amacher, S. L., B. W. Draper, B. R. Summers, and C. B. Kimmel, 2002 The zebrafish T-box genes no tail and spadetail are required for development of trunk and tail mesoderm and medial floor plate. Development 129: 3311–3323.

Amaya, E., T. J. Musci, and M. W. Kirschner, 1991 Expression of a dominant negative mutant of the FGF receptor disrupts mesoderm formation in Xenopus embryos. Cell 66: 257–270. https://doi.org/10.1016/0092-8674(91)90616-7

Arman, E., R. Haffner-Krausz, Y. Chen, J. K. Heath, and P. Lonai, 1998 Targeted disruption of fibroblast growth factor (FGF) receptor 2 suggests a role for FGF signaling in pregastrulation mammalian development. Proc. Natl. Acad. Sci. USA 95: 5082–5087. https://doi.org/10.1073/pnas.95.9.5082

Begemann, G., and P. W. Ingham, 2000 Developmental regulation of Tbx5 in zebrafish embryogenesis. Mech. Dev. 90: 299–304. https://doi.org/10.1016/S0925-4773(99)00246-4

Bertrand, S., T. Iwema, and H. Escriva, 2014 FGF signaling emerged concomitantly with the origin of Eumetazoans. Mol. Biol. Evol. 31: 310–318. https://doi.org/10.1093/molbev/mst222

Brand, M., C. P. Heisenberg, Y. J. Jiang, D. Beuchle, K. Lun *et al.*, 1996 Mutations in zebrafish genes affecting the formation of the boundary between midbrain and hindbrain. Development 123: 179–190.

Broccoli, V., E. Boncinelli, and W. Wurst, 1999 The caudal limit of Otx2 expression positions the isthmic organizer. Nature 401: 164–168. https://doi.org/10.1038/43670

Camarata, T., J. Krcmery, D. Snyder, S. Park, J. Topczewski *et al.*, 2010 Pdlim7 (LMP4) regulation of Tbx5 specifies zebrafish heart atrio-ventricular boundary and valve formation. Dev. Biol. 337: 233–245. https://doi.org/10.1016/j.ydbio.2009.10.039

Camenisch, T. D., A. P. Spicer, T. Brehm-Gibson, J. Biesterfeldt, M. L. Augustine *et al.*, 2000 Disruption of hyaluronan synthase-2 abrogates normal cardiac morphogenesis and hyaluronan-mediated transformation of epithelium to mesenchyme. J. Clin. Invest. 106: 349–360. https://doi.org/10.1172/JCI10272

Chellaiah, A. T., D. G. McEwen, S. Werner, J. Xu, and D. M. Ornitz, 1994 Fibroblast growth factor receptor (FGFR) 3. Alternative splicing in immunoglobulin-like domain III creates a receptor highly specific for acidic FGF/FGF-1. J. Biol. Chem. 269: 11620–11627.

Cheng, X. N., M. Shao, J. T. Li, Y. F. Wang, J. Qi *et al.*, 2017 Leucine repeat adaptor protein 1 interacts with Dishevelled to regulate gastrulation cell movements in zebrafish. Nat. Commun. 8: 1353. https://doi.org/10.1038/s41467-017-01552-x

Chi, C. L., S. Martinez, W. Wurst, and G. R. Martin, 2003 The isthmic organizer signal FGF8 is required for cell survival in the prospective midbrain and cerebellum. Development 130: 2633–2644. https://doi.org/10.1242/dev.00487

Ciruna, B., and J. Rossant, 2001 FGF signaling regulates mesoderm cell fate specification and morphogenetic movement at the primitive streak. Dev. Cell 1: 37–49. https://doi.org/10.1016/S1534-5807(01)00017-X

Ciruna, B., A. Jenny, D. Lee, M. Mlodzik, and A. F. Schier, 2006 Planar cell polarity signalling couples cell division and morphogenesis during neurulation. Nature 439: 220–224. https://doi.org/10.1038/nature04375

Cohn, M. J., J. C. Izpisua-Belmonte, H. Abud, J. K. Heath, and C. Tickle, 1995 Fibroblast growth factors induce additional limb development from the flank of chick embryos. Cell 80: 739–746. https://doi.org/10.1016/0092-8674(95)90352-6

Colvin, J. S., B. A. Bohne, G. W. Harding, D. G. McEwen, and D. M. Ornitz, 1996 Skeletal overgrowth and deafness in mice lacking fibroblast growth factor receptor 3. Nat. Genet. 12: 390–397. https://doi.org/10.1038/ng0496-390

Conlon, F. L., S. G. Sedgwick, K. M. Weston, and J. C. Smith, 1996 Inhibition of Xbra transcription activation causes defects in mesodermal patterning and reveals autoregulation of Xbra in dorsal mesoderm. Development 122: 2427–2435.

Crossley, P. H., S. Martinez, and G. R. Martin, 1996a Midbrain development induced by FGF8 in the chick embryo. Nature 380: 66–68. https://doi.org/10.1038/380066a0

Crossley, P. H., G. Minowada, C. A. MacArthur, and G. R. Martin, 1996b Roles for FGF8 in the induction, initiation, and maintenance of chick limb development. Cell 84: 127–136. https://doi.org/10.1016/S0092-8674(00)80999-X

Crump, J. G., L. Maves, N. D. Lawson, B. M. Weinstein, and C. B. Kimmel, 2004a An essential role for Fgfs in endodermal pouch formation influences later craniofacial skeletal patterning. Development 131: 5703–5716. https://doi.org/10.1242/dev.01444

Crump, J. G., M. E. Swartz, and C. B. Kimmel, 2004b An integrin-dependent role of pouch endoderm in hyoid cartilage development. PLoS Biol. 2: E244. https://doi.org/10.1371/journal.pbio.0020244

Crump, J. G., M. E. Swartz, J. K. Eberhart, and C. B. Kimmel, 2006 Moz-dependent Hox expression controls segment-specific fate maps of skeletal precursors in the face. Development 133: 2661–2669. https://doi.org/10.1242/dev.02435

Dahlem, T. J., K. Hoshijima, M. J. Jurynec, D. Gunther, C. G. Starker *et al.*, 2012 Simple methods for generating and detecting locus-specific mutations induced with TALENs in the zebrafish genome. PLoS Genet. 8: e1002861. https://doi.org/10.1371/journal.pgen.1002861

Davis, R. L., and M. W. Kirschner, 2000 The fate of cells in the tailbud of Xenopus laevis. Development 127: 255–267.

de Jong, M., H. Rauwerda, O. Bruning, J. Verkooijen, H. P. Spaink *et al.*, 2010 RNA isolation method for single embryo transcriptome analysis in zebrafish. BMC Res. Notes 3: 73. https://doi.org/10.1186/1756-0500-3-73

De Moerlooze, L., B. Spencer-Dene, J. M. Revest, M. Hajihosseini, I. Rosewell *et al.*, 2000 An important role for the IIIb isoform of fibroblast growth factor receptor 2 (FGFR2) in mesenchymal-epithelial signalling during mouse organogenesis. Development 127: 483–492.

Deng, C., A. Wynshaw-Boris, F. Zhou, A. Kuo, and P. Leder, 1996 Fibroblast growth factor receptor 3 is a negative regulator of bone growth. Cell 84: 911–921. https://doi.org/10.1016/S0092-8674(00)81069-7

Deng, C. X., A. Wynshaw-Boris, M. M. Shen, C. Daugherty, D. M. Ornitz *et al.*, 1994 Murine FGFR-1 is required for early postimplantation growth and axial organization. Genes Dev. 8: 3045–3057. https://doi.org/10.1101/gad.8.24.3045

Draper, B. W., D. W. Stock, and C. B. Kimmel, 2003 Zebrafish fgf24 functions with fgf8 to promote posterior mesodermal development. Development 130: 4639–4654. https://doi.org/10.1242/dev.00671

Eberhart, J. K., M. E. Swartz, J. G. Crump, and C. B. Kimmel, 2006 Early Hedgehog signaling from neural to oral epithelium organizes anterior craniofacial development. Development 133: 1069–1077. https://doi.org/10.1242/dev.02281

El-Brolosy, M. A., Z. Kontarakis, A. Rossi, C. Kuenne, S. Gunther *et al.*, 2019 Genetic compensation triggered by mutant mRNA degradation. Nature 568: 193–197. https://doi.org/10.1038/s41586-019-1064-z

Fallon, J. F., A. Lopez, M. A. Ros, M. P. Savage, B. B. Olwin *et al.*, 1994 FGF-2: apical ectodermal ridge growth signal for chick limb development. Science 264: 104–107. https://doi.org/10.1126/science.7908145

Fischer, S., B. W. Draper, and C. J. Neumann, 2003 The zebrafish fgf24 mutant identifies an additional level of Fgf signaling involved in vertebrate forelimb initiation. Development 130: 3515–3524. https://doi.org/10.1242/dev.00537

Furthauer, M., C. Thisse, and B. Thisse, 1997 A role for FGF-8 in the dorsoventral patterning of the zebrafish gastrula. Development 124: 4253–4264.

Furthauer, M., J. Van Celst, C. Thisse, and B. Thisse, 2004 Fgf signalling controls the dorsoventral patterning of the zebrafish embryo. Development 131: 2853–2864. https://doi.org/10.1242/dev.01156

Garrity, D. M., S. Childs, and M. C. Fishman, 2002 The heartstrings mutation in zebrafish causes heart/fin Tbx5 deficiency syndrome. Development 129: 4635–4645.

Gibert, Y., A. Gajewski, A. Meyer, and G. Begemann, 2006 Induction and prepatterning of the zebrafish pectoral fin bud requires axial retinoic acid signaling. Development 133: 2649–2659. https://doi.org/10.1242/dev.02438

Giraldez, A. J., R. M. Cinalli, M. E. Glasner, A. J. Enright, J. M. Thomson *et al.*, 2005 MicroRNAs regulate brain morphogenesis in zebrafish. Science 308: 833–838. https://doi.org/10.1126/science.1109020

Grandel, H., and S. Schulte-Merker, 1998 The development of the paired fins in the zebrafish (Danio rerio). Mech. Dev. 79: 99–120. https://doi.org/10.1016/S0925-4773(98)00176-2

Grandel, H., B. W. Draper, and S. Schulte-Merker, 2000 Dackel acts in the ectoderm of the zebrafish pectoral fin bud to maintain AER signaling. Development 127: 4169–4178.

Griffin, K., R. Patient, and N. Holder, 1995 Analysis of FGF function in normal and no tail zebrafish embryos reveals separate mechanisms for formation of the trunk and the tail. Development 121: 2983–2994.

Halpern, M. E., R. K. Ho, C. Walker, and C. B. Kimmel, 1993 Induction of muscle pioneers and floor plate is distinguished by the zebrafish no tail mutation. Cell 75: 99–111. https://doi.org/10.1016/S0092-8674(05)80087-X

Harvey, S. A., and M. P. Logan, 2006 sall4 acts downstream of tbx5 and is required for pectoral fin outgrowth. Development 133: 1165–1173. https://doi.org/10.1242/dev.02259

Hino, H., A. Nakanishi, R. Seki, T. Aoki, E. Yamaha *et al.*, 2018 Roles of maternal wnt8a transcripts in axis formation in zebrafish. Dev. Biol. 434: 96–107. https://doi.org/10.1016/j.ydbio.2017.11.016

Jao, L. E., S. R. Wente, and W. Chen, 2013 Efficient multiplex biallelic zebrafish genome editing using a CRISPR nuclease system. Proc. Natl. Acad. Sci. USA 110: 13904–13909. https://doi.org/10.1073/pnas.1308335110

Johnson, D. E., J. Lu, H. Chen, S. Werner, and L. T. Williams, 1991 The human fibroblast growth factor receptor genes: a common structural arrangement underlies the mechanisms for generating receptor forms that differ in their third immunoglobulin domain. Mol. Cell. Biol. 11: 4627–4634. https://doi.org/10.1128/MCB.11.9.4627

Kanki, J. P., and R. K. Ho, 1997 The development of the posterior body in zebrafish. Development 124: 881–893.

Kawakami, Y., J. Capdevila, D. Buscher, T. Itoh, C. Rodriguez Esteban *et al.*, 2001 WNT signals control FGF-dependent limb initiation and AER induction in the chick embryo. Cell 104: 891–900. https://doi.org/10.1016/S0092-8674(01)00285-9

Kengaku, M., J. Capdevila, C. Rodriguez-Esteban, J. De La Pena, R. L. Johnson *et al.*, 1998 Distinct WNT pathways regulating AER formation and dorsoventral polarity in the chick limb bud. Science 280: 1274–1277. https://doi.org/10.1126/science.280.5367.1274

Kimelman, D., 2016 Tales of tails (and trunks): forming the posterior body in vertebrate embryos. Curr. Top. Dev. Biol. 116: 517–536. https://doi.org/10.1016/bs.ctdb.2015.12.008

Kimmel, C. B., D. A. Kane, C. Walker, R. M. Warga, and M. B. Rothman, 1989 A mutation that changes cell movement and cell fate in the zebrafish embryo. Nature 337: 358–362. https://doi.org/10.1038/337358a0

Kimmel, C. B., C. T. Miller, and C. B. Moens, 2001 Specification and morphogenesis of the zebrafish larval head skeleton. Dev. Biol. 233: 239–257. https://doi.org/10.1006/dbio.2001.0201

Koch, P., H. B. Lohr, and W. Driever, 2014 A mutation in cnot8, component of the Ccr4-not complex regulating transcript stability, affects expression levels of developmental regulators and reveals a role of Fgf3 in development of caudal hypothalamic dopaminergic neurons. PLoS One 9: e113829. https://doi.org/10.1371/journal.pone.0113829

Krauss, S., T. Johansen, V. Korzh, and A. Fjose, 1991 Expression of the zebrafish paired box gene pax[zf-b] during early neurogenesis. Development 113: 1193–1206.

Krauss, S., J. P. Concordet, and P. W. Ingham, 1993 A functionally conserved homolog of the Drosophila segment polarity gene hh is expressed in tissues with polarizing activity in zebrafish embryos. Cell 75: 1431–1444. https://doi.org/10.1016/0092-8674(93)90628-4

Larbuisson, A., J. Dalcq, J. A. Martial, and M. Muller, 2013 Fgf receptors Fgfr1a and Fgfr2 control the function of pharyngeal endoderm in late cranial cartilage development. Differentiation 86: 192–206. https://doi.org/10.1016/j.diff.2013.07.006

Laufer, E., C. E. Nelson, R. L. Johnson, B. A. Morgan, and C. Tabin, 1994 Sonic hedgehog and Fgf-4 act through a signaling cascade and feedback loop to integrate growth and patterning of the developing limb bud. Cell 79: 993–1003. https://doi.org/10.1016/0092-8674(94)90030-2

Leerberg, D. M., K. Sano, and B. W. Draper, 2017 Fibroblast growth factor signaling is required for early somatic gonad development in zebrafish. PLoS Genet. 13: e1006993. https://doi.org/10.1371/journal.pgen.1006993

Lemmon, M. A., and J. Schlessinger, 1994 Regulation of signal transduction and signal diversity by receptor oligomerization. Trends Biochem. Sci. 19: 459–463. https://doi.org/10.1016/0968-0004(94)90130-9

Liu, D. W., C. H. Hsu, S. M. Tsai, C. D. Hsiao, and W. P. Wang, 2011 A variant of fibroblast growth factor receptor 2 (Fgfr2) regulates left-right asymmetry in zebrafish. PLoS One 6: e21793. https://doi.org/10.1371/journal.pone.0021793

Lovely, C. B., M. E. Swartz, N. McCarthy, J. L. Norrie, and J. K. Eberhart, 2016 Bmp signaling mediates endoderm pouch morphogenesis by regulating Fgf signaling in zebrafish. Development 143: 2000–2011. https://doi.org/10.1242/dev.129379

Luo, Y., W. Lu, K. A. Mohamedali, J. H. Jang, R. B. Jones *et al.*, 1998 The glycine box: a determinant of specificity for fibroblast growth factor. Biochemistry 37: 16506–16515. https://doi.org/10.1021/bi9816599

Ma, Z., P. Zhu, H. Shi, L. Guo, Q. Zhang *et al.*, 2019 PTC-bearing mRNA elicits a genetic compensation response via Upf3a and COMPASS components. Nature 568: 259–263. https://doi.org/10.1038/s41586-019-1057-y

Manfroid, I., F. Delporte, A. Baudhuin, P. Motte, C. J. Neumann *et al.*, 2007 Reciprocal endoderm-mesoderm interactions mediated by fgf24 and fgf10 govern pancreas development. Development 134: 4011–4021. https://doi.org/10.1242/dev.007823

Marin, F., and L. Puelles, 1994 Patterning of the embryonic avian midbrain after experimental inversions: a polarizing activity from the isthmus. Dev. Biol. 163: 19–37. https://doi.org/10.1006/dbio.1994.1120

Martínez, S., F. Marin, M. A. Nieto, and L. Puelles, 1995 Induction of ectopic engrailed expression and fate change in avian rhombomeres: intersegmental boundaries as barriers. Mech. Dev. 51: 289–303. https://doi.org/10.1016/0925-4773(95)00376-2

McCarthy, N., A. Sidik, J. Y. Bertrand, and J. K. Eberhart, 2016 An Fgf-Shh signaling hierarchy regulates early specification of the zebrafish skull. Dev. Biol. 415: 261–277. https://doi.org/10.1016/j.ydbio.2016.04.005

Mercader, N., 2007 Early steps of paired fin development in zebrafish compared with tetrapod limb development. Dev. Growth Differ. 49: 421–437. https://doi.org/10.1111/j.1440-169X.2007.00942.x

Meyers, E. N., M. Lewandoski, and G. R. Martin, 1998 An Fgf8 mutant allelic series generated by Cre- and Flp-mediated recombination. Nat. Genet. 18: 136–141. https://doi.org/10.1038/ng0298-136

Mikkola, I., A. Fjose, J. Y. Kuwada, S. Wilson, P. H. Guddal *et al.*, 1992 The paired domain-containing nuclear factor pax[b] is expressed in specific commissural interneurons in zebrafish embryos. J. Neurobiol. 23: 933–946. https://doi.org/10.1002/neu.480230802

Millen, K. J., W. Wurst, K. Herrup, and A. L. Joyner, 1994 Abnormal embryonic cerebellar development and patterning of postnatal foliation in two mouse Engrailed-2 mutants. Development 120: 695–706.

Millet, S., K. Campbell, D. J. Epstein, K. Losos, E. Harris *et al.*, 1999 A role for Gbx2 in repression of Otx2 and positioning the mid/hindbrain organizer. Nature 401: 161–164. https://doi.org/10.1038/43664

Min, H., D. M. Danilenko, S. A. Scully, B. Bolon, B. D. Ring *et al.*, 1998 Fgf-10 is required for both limb and lung development and exhibits striking functional similarity to Drosophila branchless. Genes Dev. 12: 3156–3161. https://doi.org/10.1101/gad.12.20.3156

Mohammadi, M., S. K. Olsen, and O. A. Ibrahimi, 2005 Structural basis for fibroblast growth factor receptor activation. Cytokine Growth Factor Rev. 16: 107–137. https://doi.org/10.1016/j.cytogfr.2005.01.008

Moreno-Mateos, M. A., C. E. Vejnar, J. D. Beaudoin, J. P. Fernandez, E. K. Mis *et al.*, 2015 CRISPRscan: designing highly efficient sgRNAs for CRISPR-Cas9 targeting in vivo. Nat. Methods 12: 982–988. https://doi.org/10.1038/nmeth.3543

Mork, L., and G. Crump, 2015 Zebrafish craniofacial development: a window into early patterning. Curr. Top. Dev. Biol. 115: 235–269. https://doi.org/10.1016/bs.ctdb.2015.07.001

Mou, H., J. L. Smith, L. Peng, H. Yin, J. Moore *et al.*, 2017 CRISPR/Cas9-mediated genome editing induces exon skipping by alternative splicing or exon deletion. Genome Biol. 18: 108. https://doi.org/10.1186/s13059-017-1237-8

Münchberg, S. R., E. A. Ober, and H. Steinbeisser, 1999 Expression of the Ets transcription factors erm and pea3 in early zebrafish development. Mech. Dev. 88: 233–236. https://doi.org/10.1016/S0925-4773(99)00179-3

Nechiporuk, A., T. Linbo, and D. W. Raible, 2005 Endoderm-derived Fgf3 is necessary and sufficient for inducing neurogenesis in the epibranchial placodes in zebrafish. Development 132: 3717–3730. https://doi.org/10.1242/dev.01876

Neumann, C. J., H. Grandel, W. Gaffield, S. Schulte-Merker, and C. Nusslein-Volhard, 1999 Transient establishment of anteroposterior polarity in the zebrafish pectoral fin bud in the absence of sonic hedgehog activity. Development 126: 4817–4826.

Ng, J. K., Y. Kawakami, D. Buscher, A. Raya, T. Itoh *et al.*, 2002 The limb identity gene Tbx5 promotes limb initiation by interacting with Wnt2b and Fgf10. Development 129: 5161–5170.

Niswander, L., and G. R. Martin, 1992 Fgf-4 expression during gastrulation, myogenesis, limb and tooth development in the mouse. Development 114: 755–768.

Nomura, R., E. Kamei, Y. Hotta, M. Konishi, A. Miyake *et al.*, 2006 Fgf16 is essential for pectoral fin bud formation in zebrafish. Biochem. Biophys. Res. Commun. 347: 340–346. https://doi.org/10.1016/j.bbrc.2006.06.108

Norton, W. H., J. Ledin, H. Grandel, and C. J. Neumann, 2005 HSPG synthesis by zebrafish Ext2 and Extl3 is required for Fgf10 signalling during limb development. Development 132: 4963–4973. https://doi.org/10.1242/dev.02084

Ornitz, D. M., and N. Itoh, 2001 Fibroblast growth factors. Genome Biol. 2: REVIEWS3005.

Ornitz, D. M., J. Xu, J. S. Colvin, D. G. McEwen, C. A. MacArthur *et al.*, 1996 Receptor specificity of the fibroblast growth factor family. J. Biol. Chem. 271: 15292–15297. https://doi.org/10.1074/jbc.271.25.15292

Ota, S., N. Tonou-Fujimori, N. Tonou-Fujimori, Y. Nakayama, Y. Ito *et al.*, 2010 FGF receptor gene expression and its regulation by FGF signaling during early zebrafish development. Genesis 48: 707–716. https://doi.org/10.1002/dvg.20682

Pawson, T., 1995 Protein modules and signalling networks. Nature 373: 573–580. https://doi.org/10.1038/373573a0

Powers, C. J., S. W. McLeskey, and A. Wellstein, 2000 Fibroblast growth factors, their receptors and signaling. Endocr. Relat. Cancer 7: 165–197. https://doi.org/10.1677/erc.0.0070165

R Core Team, 2015 *R: A Language and Environment for Statistical Computing*. R Foundation for Statistical Computing, Vienna.

Reifers, F., H. Bohli, E. C. Walsh, P. H. Crossley, D. Y. Stainier *et al.*, 1998 Fgf8 is mutated in zebrafish acerebellar (ace) mutants and is required for maintenance of midbrain-hindbrain boundary development and somitogenesis. Development 125: 2381–2395.

Rice, R., B. Spencer-Dene, E. C. Connor, A. Gritli-Linde, A. P. McMahon *et al.*, 2004 Disruption of Fgf10/Fgfr2b-coordinated epithelial-mesenchymal interactions causes cleft palate. J. Clin. Invest. 113: 1692–1700. https://doi.org/10.1172/JCI20384

Rohner, N., M. Bercsenyi, L. Orban, M. E. Kolanczyk, D. Linke *et al.*, 2009 Duplication of fgfr1 permits Fgf signaling to serve as a target for selection during domestication. Curr. Biol. 19: 1642–1647. https://doi.org/10.1016/j.cub.2009.07.065

Rohs, P., A. M. Ebert, A. Zuba, and S. McFarlane, 2013 Neuronal expression of fibroblast growth factor receptors in zebrafish.

Gene Expr. Patterns 13: 354–361. https://doi.org/10.1016/j.gep.2013.06.006
Rossi, A., Z. Kontarakis, C. Gerri, H. Nolte, S. Holper *et al.*, 2015 Genetic compensation induced by deleterious mutations but not gene knockdowns. Nature 524: 230–233. https://doi.org/10.1038/nature14580
Schier, A. F., and W. S. Talbot, 2005 Molecular genetics of axis formation in zebrafish. Annu. Rev. Genet. 39: 561–613. https://doi.org/10.1146/annurev.genet.37.110801.143752
Schilling, T. F., and C. B. Kimmel, 1994 Segment and cell type lineage restrictions during pharyngeal arch development in the zebrafish embryo. Development 120: 483–494.
Scholpp, S., C. Groth, C. Lohs, M. Lardelli, and M. Brand, 2004 Zebrafish fgfr1 is a member of the fgf8 synexpression group and is required for fgf8 signalling at the midbrain-hindbrain boundary. Dev. Genes Evol. 214: 285–295. https://doi.org/10.1007/s00427-004-0409-1
Schulte-Merker, S., R. K. Ho, B. G. Herrmann, and C. Nusslein-Volhard, 1992 The protein product of the zebrafish homologue of the mouse T gene is expressed in nuclei of the germ ring and the notochord of the early embryo. Development 116: 1021–1032.
Shah, A. N., C. B. Moens, and A. C. Miller, 2016 Targeted candidate gene screens using CRISPR/Cas9 technology. Methods Cell Biol. 135: 89–106. https://doi.org/10.1016/bs.mcb.2016.01.008
Sharpe, J. J., and T. A. Cooper, 2017 Unexpected consequences: exon skipping caused by CRISPR-generated mutations. Genome Biol. 18: 109. https://doi.org/10.1186/s13059-017-1240-0
Sleptsova-Friedrich, I., Y. Li, A. Emelyanov, M. Ekker, V. Korzh *et al.*, 2001 fgfr3 and regionalization of anterior neural tube in zebrafish. Mech. Dev. 102: 213–217. https://doi.org/10.1016/S0925-4773(01)00280-5
Sun, X., E. N. Meyers, M. Lewandoski, and G. R. Martin, 1999 Targeted disruption of Fgf8 causes failure of cell migration in the gastrulating mouse embryo. Genes Dev. 13: 1834–1846. https://doi.org/10.1101/gad.13.14.1834
Sun, X., F. V. Mariani, and G. R. Martin, 2002 Functions of FGF signalling from the apical ectodermal ridge in limb development. Nature 418: 501–508. https://doi.org/10.1038/nature00902
Swartz, M. E., K. Sheehan-Rooney, M. J. Dixon, and J. K. Eberhart, 2011 Examination of a palatogenic gene program in zebrafish. Dev. Dyn. 240: 2204–2220. https://doi.org/10.1002/dvdy.22713
Thisse, B., S. Pflumio, M. Fürthauer, B. Loppin, V. Heyer *et al.*, 2001 *Expression of the Zebrafish Genome During Embryogenesis*. ZFIN Direct Data Submission, Eugene, OR.
Thisse, B., G. J. Wright, and C. Thisse, 2008 *Embryonic and Larval Expression Patterns from a Large Scale Screening for Novel Low Affinity Extracellular Protein Interactions*. ZFIN Direct Data Submission, Eugene, OR.
Thisse, C., and B. Thisse, 2005 *High Throughput Expression Analysis of ZF-Models Consortium Clones*. ZFIN Direct Data Submission, Eugene, OR.
Tonou-Fujimori, N., M. Takahashi, H. Onodera, H. Kikuta, S. Koshida *et al.*, 2002 Expression of the FGF receptor 2 gene (fgfr2) during embryogenesis in the zebrafish Danio rerio. Mech. Dev. 119: S173–S178. https://doi.org/10.1016/S0925-4773(03)00112-6
Trokovic, R., N. Trokovic, S. Hernesniemi, U. Pirvola, D. M. Vogt Weisenhorn *et al.*, 2003 FGFR1 is independently required in both developing mid- and hindbrain for sustained response to isthmic signals. EMBO J. 22: 1811–1823. https://doi.org/10.1093/emboj/cdg169
Wada, N., Y. Javidan, S. Nelson, T. J. Carney, R. N. Kelsh *et al.*, 2005 Hedgehog signaling is required for cranial neural crest morphogenesis and chondrogenesis at the midline in the zebrafish skull. Development 132: 3977–3988. https://doi.org/10.1242/dev.01943
Wagner, D. S., and M. C. Mullins, 2002 Modulation of BMP activity in dorsal-ventral pattern formation by the chordin and ogon antagonists. Dev. Biol. 245: 109–123. https://doi.org/10.1006/dbio.2002.0614
Walker, M. B., C. T. Miller, J. Coffin Talbot, D. W. Stock, and C. B. Kimmel, 2006 Zebrafish furin mutants reveal intricacies in regulating Endothelin1 signaling in craniofacial patterning. Dev. Biol. 295: 194–205. https://doi.org/10.1016/j.ydbio.2006.03.028
Warga, R. M., R. L. Mueller, R. K. Ho, and D. A. Kane, 2013 Zebrafish Tbx16 regulates intermediate mesoderm cell fate by attenuating Fgf activity. Dev. Biol. 383: 75–89. https://doi.org/10.1016/j.ydbio.2013.08.018
Waskiewicz, A. J., H. A. Rikhof, and C. B. Moens, 2002 Eliminating zebrafish pbx proteins reveals a hindbrain ground state. Dev. Cell 3: 723–733. https://doi.org/10.1016/S1534-5807(02)00319-2
Weinberg, E. S., M. L. Allende, C. S. Kelly, A. Abdelhamid, T. Murakami *et al.*, 1996 Developmental regulation of zebrafish MyoD in wild-type, no tail and spadetail embryos. Development 122: 271–280.
Weinstein, M., X. Xu, K. Ohyama, and C. X. Deng, 1998 FGFR-3 and FGFR-4 function cooperatively to direct alveogenesis in the murine lung. Development 125: 3615–3623.
Werner, S., D. S. Duan, C. de Vries, K. G. Peters, D. E. Johnson *et al.*, 1992 Differential splicing in the extracellular region of fibroblast growth factor receptor 1 generates receptor variants with different ligand-binding specificities. Mol. Cell. Biol. 12: 82–88. https://doi.org/10.1128/MCB.12.1.82
Westerfield, M., 2000 *The Zebrafish Book. A Guide for the Laboratory Use of Zebrafish (Danio rerio)*. University of Oregon Press, Eugene, OR.
Wickham, H., 2009 *ggplot2: Elegant Graphics for Data Analysis*. Springer-Verlag, New York.
Xu, X., M. Weinstein, C. Li, M. Naski, R. I. Cohen *et al.*, 1998 Fibroblast growth factor receptor 2 (FGFR2)-mediated reciprocal regulation loop between FGF8 and FGF10 is essential for limb induction. Development 125: 753–765.
Xu, X., C. Li, K. Takahashi, H. C. Slavkin, L. Shum *et al.*, 1999a Murine fibroblast growth factor receptor 1alpha isoforms mediate node regression and are essential for posterior mesoderm development. Dev. Biol. 208: 293–306. https://doi.org/10.1006/dbio.1999.9227
Xu, X., M. Weinstein, C. Li, and C. Deng, 1999b Fibroblast growth factor receptors (FGFRs) and their roles in limb development. Cell Tissue Res. 296: 33–43. https://doi.org/10.1007/s004410051264
Yamaguchi, T. P., K. Harpal, M. Henkemeyer, and J. Rossant, 1994 fgfr-1 is required for embryonic growth and mesodermal patterning during mouse gastrulation. Genes Dev. 8: 3032–3044. https://doi.org/10.1101/gad.8.24.3032
Yayon, A., Y. Zimmer, G. H. Shen, A. Avivi, Y. Yarden *et al.*, 1992 A confined variable region confers ligand specificity on fibroblast growth factor receptors: implications for the origin of the immunoglobulin fold. EMBO J. 11: 1885–1890. https://doi.org/10.1002/j.1460-2075.1992.tb05240.x
Yeh, B. K., M. Igarashi, A. V. Eliseenkova, A. N. Plotnikov, I. Sher *et al.*, 2003 Structural basis by which alternative splicing confers specificity in fibroblast growth factor receptors. Proc. Natl. Acad. Sci. USA 100: 2266–2271. https://doi.org/10.1073/pnas.0436500100
Yu, K., K. Karuppaiah, and D. M. Ornitz, 2015 Mesenchymal fibroblast growth factor receptor signaling regulates palatal shelf elevation during secondary palate formation. Dev. Dyn. 244: 1427–1438. https://doi.org/10.1002/dvdy.24319
Zhang, J., D. W. Houston, M. L. King, C. Payne, C. Wylie *et al.*, 1998 The role of maternal VegT in establishing the primary germ layers in Xenopus embryos. Cell 94: 515–524. https://doi.org/10.1016/S0092-8674(00)81592-5

Zhang, X., O. A. Ibrahimi, S. K. Olsen, H. Umemori, M. Mohammadi *et al.*, 2006 Receptor specificity of the fibroblast growth factor family. The complete mammalian FGF family. J. Biol. Chem. 281: 15694–15700. https://doi.org/10.1074/jbc.M601252200

Zhao, H., T. Yang, B. P. Madakashira, C. A. Thiels, C. A. Bechtle *et al.*, 2008 Fibroblast growth factor receptor signaling is essential for lens fiber cell differentiation. Dev. Biol. 318: 276–288. https://doi.org/10.1016/j.ydbio.2008.03.028

Zuniga, A., 2015 Next generation limb development and evolution: old questions, new perspectives. Development 142: 3810–3820. https://doi.org/10.1242/dev.125757

Communicating editor: D. Greenstein